Straight Interference Pattern to Curved-Expanded-Inclined Interference Pattern—Static to Dynamic Double Slit/Cross-Double Slit Experiments

hui peng (davidpeng1749@gmail.com)

Research Article

Keywords: double slit experiments, cross-double slit experiments, interference pattern, light bending, curved interference pattern, expanded interference pattern, inclined interference pattern

Posted Date: August 30th, 2021

DOI: https://doi.org/10.21203/rs.3.rs-846260/v1

EDITORIAL NOTE:

Expression of Concern: Research Square has detected high levels of self-ciation in this preprint

Straight Interference Pattern to Curved-Expanded-Inclined Interference Pattern

---Static to Dynamic Double Slit/Cross-Double Slit Experiments

Hui Peng

Email: davidpeng1749@gmail.com

Abstract In this article, we show three novel universal phenomena of the double slit, cross-double slit and grating experiments: (1) the interference patterns can curve; (2) the interference patterns can expand; and (3) the interference patterns created by the tilt double slits can inclined to the axis that is perpendicular to the axis the diaphragm rotates around. The directions of the patterns curved towards are determined by how the diaphragm rotates, i.e., clockwise or counterclockwise. To determine the directions, we proposed Right-hand rule and Left-hand rule. The magnitudes of three phenomena depend on the direction of the rotation and two angles: the original angle of the double slit on the diaphragm relative to the rotation axis and the angle the diaphragm rotates. We derived the formular to calculate the expansion of the patterns, and the formular to calculate the inclination angle of patterns. In the regular double slit experiment, photons need to know whether there is a double slit or not. Now, photons need to know: (1) the orientation of the double slit; (2) which axis the diaphragm rotating around; (3) the direction of rotation, i.e., clockwise or counterclockwise; (4) the angle of the rotation. The Feynman's mystery of the double slit is more mysterious.

Keywords: double slit experiments, cross-double slit experiments, interference pattern, light bending, curved interference pattern, expanded interference pattern, inclined interference pattern

Declaration: author declares that there is no interesting conflict.

Content

1. Introduction
2. Apparatus
3. Experiments of Double Slit
    3.1. Curved Interference Patterns
    3.2. Expanded Interference Patterns
    3.3. Curved, Expanded and Inclined Interference Patterns
4. Experiments of Cross-Double Slit
    4.1. Curved and Expanded Interference Patterns
    4.2. Curved, Expanded and Inclined Interference Patterns

5. Experiments of Grating
5.1. Curved Interference Patterns
5.2. Expanded Interference Patterns
5.3. Curved, Expanded and Inclined Interference Patterns
6. Description
6.1. Right-hand Rule and Left-hand Rule for Curved Interference Patterns
6.2. Formular for Expanded Interference Patterns
6.3. Formular for Inclined Interference Patterns
7. Experiments: Particle or Wave
7.1. Blocking Curved Interference Patterns
7.2. Blocking Expanded Interference Patterns
7.3. Blocking Inclined Interference Patterns
8. Discussion
8.1. Static Double Slit Experiments vs Dynamic Double Slit Experiments
8.2. On Light Bending
9. Summery
Appendixes:
(A1) Expanded Pattern of Disc-ring experiments
(A2) Curved, Expanded and Inclined Pattern of More Cross-Double Slit Experiments
(A3) Link of Video-1: Evolution of curved interference patterns
(A4) Link of Video-2: Evolution of expanded interference patterns
(A5) Link of Video-3: Evolution of curved, expanded and inclined interference patterns

1. Introduction

The light beams are bended mainly in four phenomena, (A) light refraction, (B) light bended by gravity, (C) Talbot effect, (D) Airy beam curves. We group those four phenomena into two categories.

First category: the light beam is bended entirely, which contains:

(A) light refraction: attributing to the different refractive indexes (Snell–Descartes law), the light beam bends when it passes the interface between two mediums [1]; and

(B) Gravity bends light: this phenomenon was predicted by Einstein [2]. In 1919, the observation of eclipse shown that the light beam of a star was bended by gravity of Sun to propagate along curved trajectories. The more phenomena of the gravitational lens are observed.

Second category: the diffraction patterns and interfering waves are bended, which contains:

(C) Talbot effect in which certain diffraction patterns distribute along tilted lines. The phenomenon was first discovered by Talbot in 1836 [3], and explained as phenomenon of diffraction by Rayleigh in 1881 [4]; to review, see, e.g., [5];

(D) Airy beam curves transversely (or self-accelerating): The interfered light waves show on curved lines. In 1979, the novel phenomenon of curved Airy beam was predicted theoretically based on Schrödinger's equation [6]. In 2007, the experiments confirmed the phenomena [7] [8], in which Airy beam transversely accelerates during propagations without external cause. In other word, Airy beam is curved/bended, or it is self-accelerating. The phenomena are also interpreted by Maxwell's equation [9], and experiments supported the theory [10]. There are review articles, e.g., [11] and [12], to name two. The phenomena of curved Airy beam have attracted considerable attentions not only because its significance in fundamental and experimental optics, but also in varieties of applications.

In this article, we show the novel phenomena of the curved-light [13], i.e., the interference patterns of the double slit, cross-double slit and grating experiments are curved transversely, i.e., the fringes distribute along curves, which is significantly different from the both the Talbot effect and the curved Airy beam. The curved interference patterns are caused by the different orientations of the diaphragms of the double slit, cross-double slit and grating.

Furthermore, we show, the first time, that the interference patterns are expanded and inclined. The new phenomena show that the characteristics of the interference patterns depend on the orientations of the diaphragms of the double slit, cross-double slit [14] and grating.

Table 1 Normal/Static Double Slit vs Novel/Dynamic Double Slit/Cross-Double Slit Experiments

	Static Pattern of Double Slit	Dynamic patterns of Novel Double Slit/Cross-Double Slit/Grating
Style of interference pattern	straight line	Curved line [13]
Change of style	No change	Bended Continuously/transversely
Distance between fringes	No change	Expand continuously [14]
Direction of patten	No change	Inclined continuously [14]
Theory	Optics, probability wave, trajectory theory	Under development

Table 1 shows the comparison between the static interference pattern of the normal double slit experiments and the dynamic interference pattern of the novel double slit and cross-double slit experiments. Here we referred the no-change interference pattern as the static pattern, while the continuously curved, expanded and incline pattern as the dynamic pattern.

Young's double slit experiment was performed in 1801 [15] [16], which, 100 years later, led to wave-particle duality. Feynman called it "a phenomenon […] has in it the heart of quantum mechanics. In reality, it contains the only mystery [of quantum mechanics]" [17]. Moreover, the nature of photons truly puzzled Einstein. He wrote to M. Besso: "All these 50 years of conscious brooding have brought me no nearer to the answer to the question: What are light quanta?" [18].

The novel phenomena of the curved, expanded and inclined interference patterns provide the comprehensive data/information to study the mystery of double slit experiments.

2. Apparatuses

The experimental apparatus contains a laser source, a protractor and the diaphragms of the cross-double slit (Figure 1a) [19] [20], double slit (Figure 1b) and grating (Figure 1c).

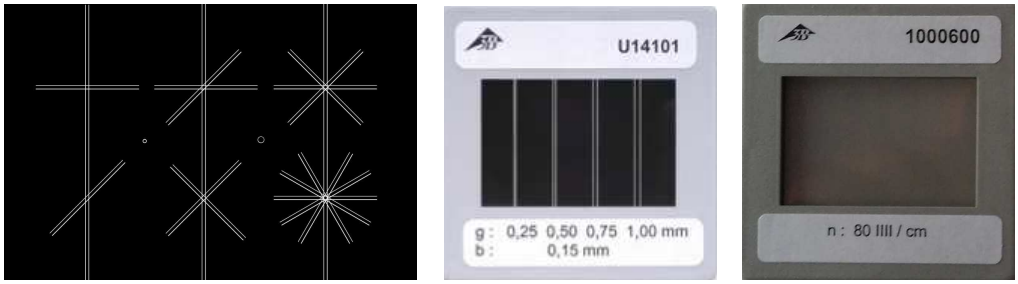

. (a) (b) (c)

Figure 1 Apparatus

3. Experiments of Double Slit

3.1. Novel Phenomena: Curved Interference Patterns

Let us start with a schematic drawing (Figure 2). The double-slit-AB is in the y-z plane, its normal vector is along the x-axis. Slit A and slit B are along the z-direction. Photons travel towards the negative x-direction.

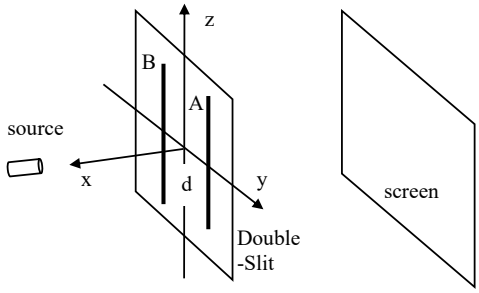

Figure 2 Standard diaphragm of double slit and its pattern

We are interested in how the interference patterns vary with different orientations of the diaphragm of double slit/cross-double slit. The novel phenomenon of the curved interference patterns is attribute to the rotations of the diaphragms around Y-axis.

An un-emphasized fact is that the interference patterns of the double slit are along straight line. On the contrary, when the diaphragm in Figure 2 rotates around Y-axis, the double slit creates the curved interference patterns as shown below.

Rotating the double slit-AB clockwise around Y-axis with different discrete angles, 45^0 (Figure 3b), 60^0 (Figure 3c) and 75^0 (Figure 3d). The original orientation corresponds to 0^0 rotation (Figure 3a).

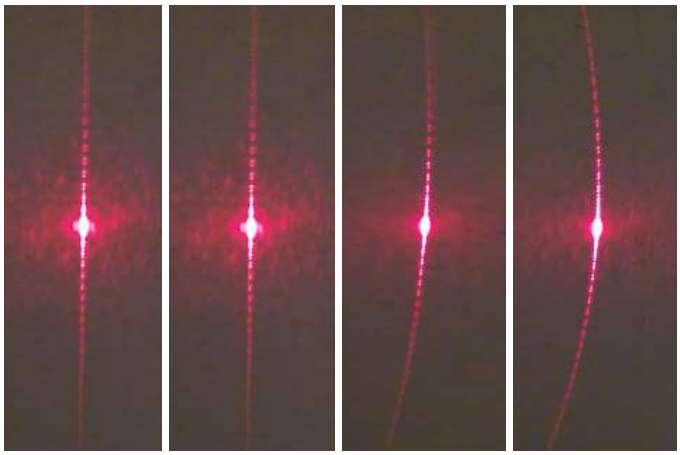

.(a) (b) (c) (d)

Figure 3 Curved Interference patterns

Observation (Figure 3): the interference patterns curved towards the left side.

Next step, back to the original orientation and rotating the double slit counterclockwise with different discrete angles (Figure 4): 45^0 (Figure 4a), 60^0 (Figure 4b) and 75^0 (Figure 4c).

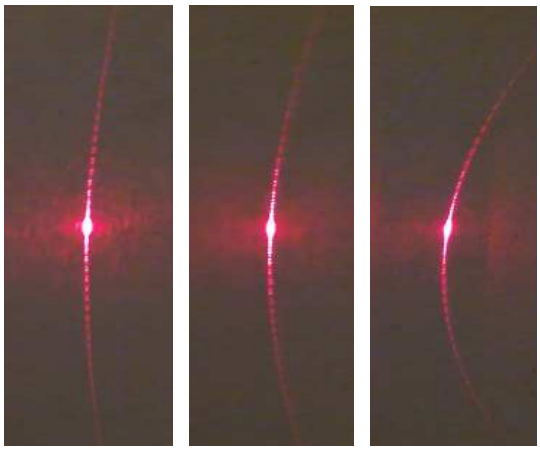

.(a) (b) (c)

Figure 4 Curved Interference patterns

Observation: the interference patterns curved towards the right side that is opposite to that of the curved interference pattern created by rotating the double slit clockwise.

Note that the degree of bending is a function of "m", where "m" is the m^{th}-order of the fringe, the bigger "m", the larger transvers distance of the pattern curved [21].

Conclusion: the photons' behaviors are so different when the diaphragm rotates: (1) clockwise or counterclockwise; (2) different angles. The larger the rotation angle, the larger curvature of the interference patterns.

3.2. Novel Phenomena: Expanded Interference Patterns

The standard optical equation describing the interference pattern of the double slit experiments relates the positions y_{const} of fringes, wave length λ, the spacing d between two slits and distance L from the double slit to detector/screen as $y_{const} = m\frac{\lambda}{d}L$. This equation was derived for the situation that the light beam is perpendicular to the plane of the double slit, denoted it as the original orientation.

Let us start with a schematic drawing (Figure 2). The coordinates of slit-A and slit-B are $y_A = d/2$ and $y_B = -d/2$, the spacing between slits A and B is "d".

We are interested in how the interference patterns vary with different orientations of the diaphragm of double slit. In this section, we study the orientation dependence of the interference patterns of the double-slit, when the diaphragm rotates around Z-axis.

The interference pattern of the double slit at the original position, $\angle a = 0^0$, is shown in Figure 5.

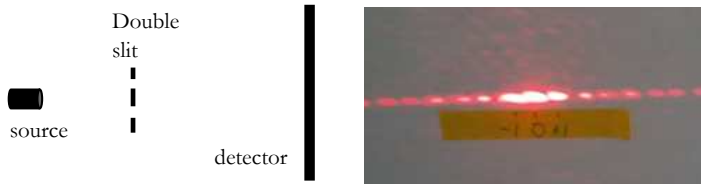

Figure 5 Diaphragm rotating 0 degree and its pattern

Then, the diaphragm rotates $\angle a = 45^0$ from the original orientation (Figure 6).

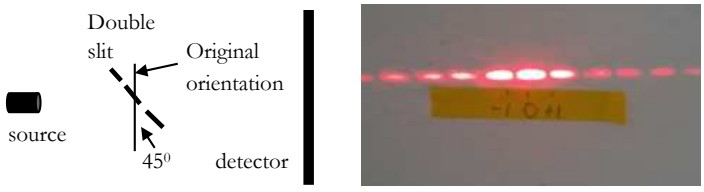

Figure 6 The diaphragm rotates 45^0

Observation: the distance between two fringes becomes longer.

The diaphragm rotates $\angle a = 60^0$ from the original orientation (Figure 7).

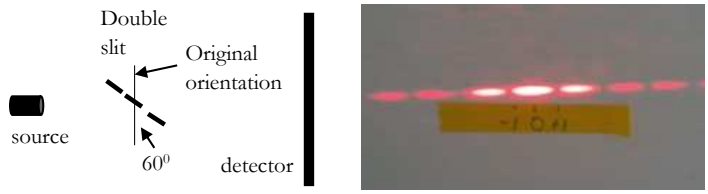

Figure 7 The diaphragm rotates 60^0

Observation: the distance between two fringes becomes longer.

The diaphragm rotates $\angle a = 75^0$ from the original orientation (Figure 8).

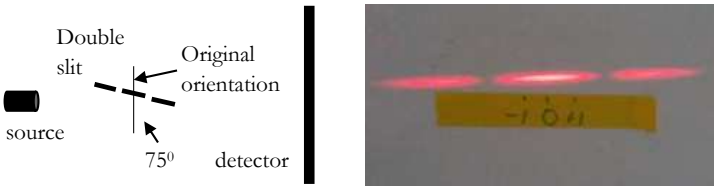

Figure 8 The diaphragm rotates 75 degrees

Observation: the distance between two fringes becomes longer.

Conclusion: (1) Figure 6 to figure 8 show the evolution of the interference patterns varying with orientations of the diaphragm rotating around the z-axis: the larger the rotation angle, the larger the expansion; (2) rotating the diaphragm clockwise and counterclockwise show the same interference patterns.

We show, the first time, that the spacings between fringes have expanded attributing to the rotation of the diaphragm.

3.3. **Novel Phenomena: Curved, Expanded and Inclined Interference Patterns**

We show the novel double slit experiments in which the following three phenomena emerged simultaneously in the same experiment: (1) the interference patterns inclined; (2) the interference patterns curved; (3) the interference patterns expanded.

To study, we setup the diaphragm of the tilt double slit in two original orientations:

First original orientation: the diaphragm is in the Y-Z-plane, X-axis is along the normal vector of the plane of the diaphragm, the source is on X-axis; the angle between the double slit and Y-axis is 45^0 clockwise (Figure 9).

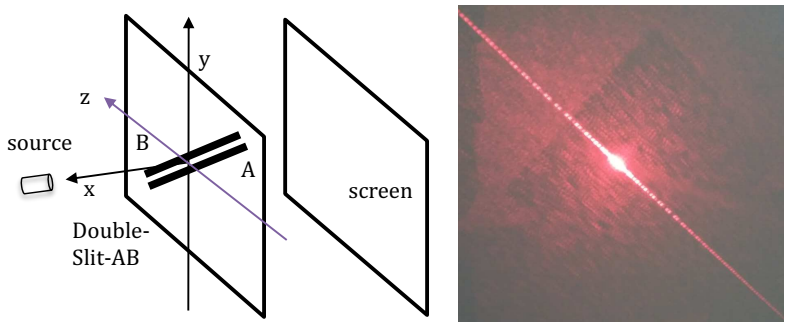

.(a) (b)

Figure 9 Diaphragm of First Orientation (a) and Original Interference Pattern-1 (b)

Second original orientation: the angle between the double slit and Y-axis is 45^0 counterclockwise (Figure 10).

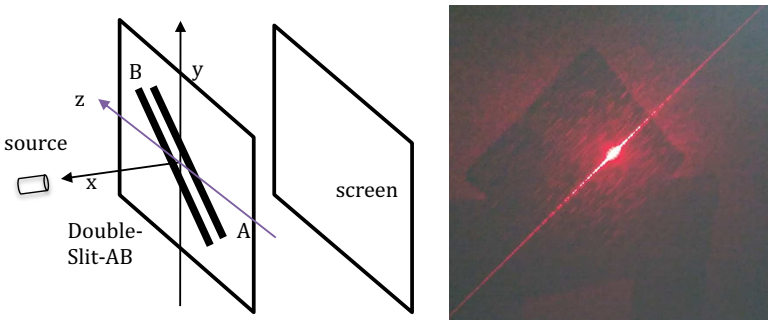

.(a) (b)

Figure 10 Diaphragm of Second Orientation (a) and Original Interference Pattern-2 (b)

3.3.1. Experiments with First Original Orientation

With the setup of First original orientation (Figure 9), we perform the experiments in two steps.

First step: rotating the diaphragm 60^0 and 75^0 around Y-axis counterclockwise (Figure 11).

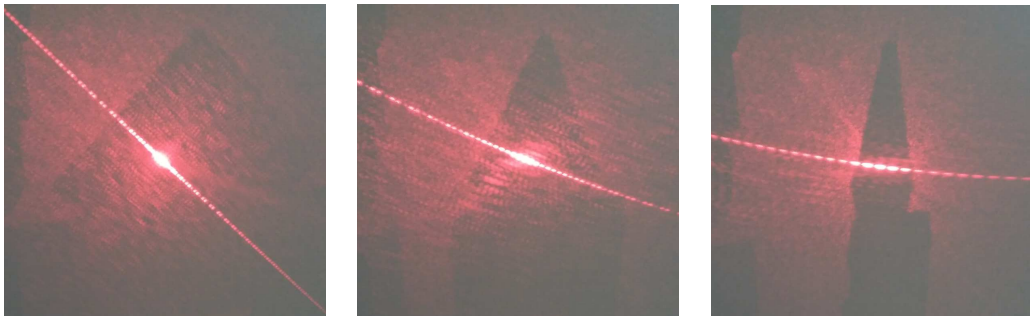

. (a) (b) (c)

Figure 11 Rotating diaphragm around Y-axis counterclockwise: (a) 0^0; (b) 60^0; (c) 75^0

Observation (Figure 11b and 11c): the large the rotation angle of the diaphragm, the larger the expansion of the distance between the fringes, curved more, and inclined more to the horizontal axis. The interference pattern curved upwards.

Second step: rotating the diaphragm 60^0 and 75^0 around Y-axis clockwise (Figure 12).

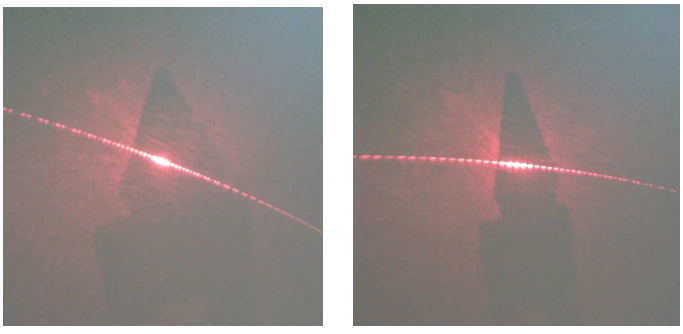

. (a) (b)

Figure 12 Rotating diaphragm around Y-axis clockwise: (a) 60^0; (b) 75^0

Observation (Figure 12a and 12b): the large the rotation angle of the diaphragm, the larger the expansion of the distance between the fringes, curved more, and inclined more towards the horizontal

axis. The interference pattern curved downwards.

3.3.2. Experiments with Second Original Orientation

With the setup of Second original orientation, we do experiments in two steps.

First step: rotating the diaphragm 60^0 and 75^0 around Y-axis counterclockwise (Figure 13).

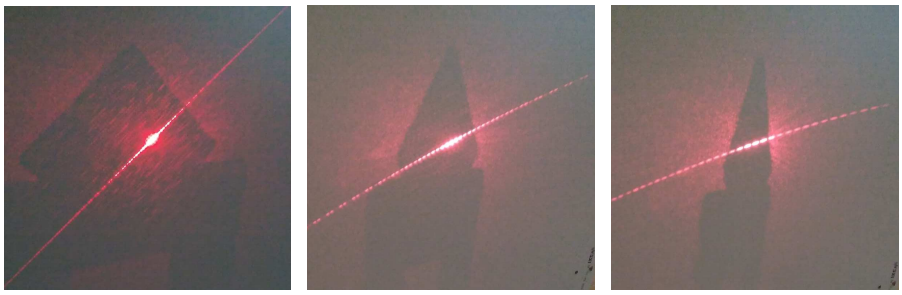

.(a) (b) (c)

Figure 13 Rotating diaphragm around Y-axis counterclockwise: (a) 0^0; (b) 60^0; (c) 75^0

Observation (Figure 13b and 13c): the large the rotation angle of the diaphragm, the larger the expansion of the distances between the fringes, curved more, and inclined more towards the horizontal axis. The interference pattern curved downwards.

Second step: rotating the diaphragm 60^0 and 75^0 respectively around Y-axis clockwise (Figure 14).

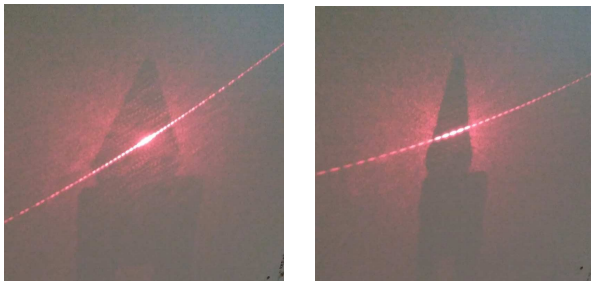

.(a) (b)

Figure 14 Rotating diaphragm around Y-axis clockwise: (a) 60^0; (b) 75^0

Observation (Figure 14a and 14b): the large the rotation angle of the diaphragm, the larger the expansion of the distances between the fringes, curved more, and inclined more towards the horizontal axis. The interference pattern curved upwards.

Conclusion: By rotating continuously the diaphragm of the tilt double slit around one axis, we observed three phenomena simultaneously in the same experiment. The interference patterns curved, expanded and inclined continuously (see attached Appendix-5: Video).

Discussion: in the regular double slit experiment, photons only need to know one factor to behave accordingly: whether there is a double slit or not. Now we show that photons need to know more factors: (1) the orientation of the double slit on the diaphragm; (2) which axis the diaphragm rotating around; (3) the direction of rotation, i.e., clockwise or counterclockwise; (4) the angle of the rotation.

To determine the directions the interference patters curved towards, Right-hand rule and Left-hand rule have been proposed [22]. A mathematical formular was derived to describe the inclination [23].

4. Experiments of Cross-Double Slit

4.1. Curved and Expanded Interference Patterns: Taking Place Simultaneously

Let us study the orientation-dependence of the interference patterns of the cross-double slit rotating around Z-axis. The apparatus consists of source, cross-double-slit, protractor and screen.

Utilizing a simple cross-double slit that consists of double-slit-AB and double-slit-CD, and double-slit-AB is perpendicular to double-slit-CD (Figure 15).

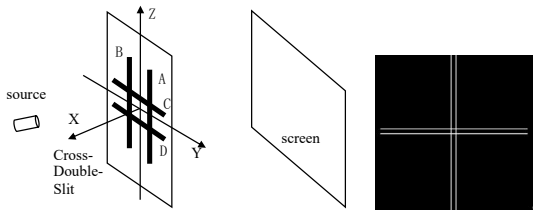

Figure 15 Cross-double-slit rotating around z-axis

Each double slit of the cross-double slit creates the interference pattern independently [19]. The pattern of the cross-double slit-ABCD is the combination of two interference patterns created respectively by the double slit-AB and double slit-CD. Figure 16 shows the 2D-interference pattern created by the cross-double slit-ABCD at the original orientation.

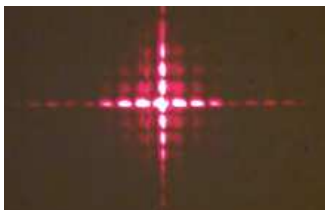

Figure 16 Diaphragm at 0^0

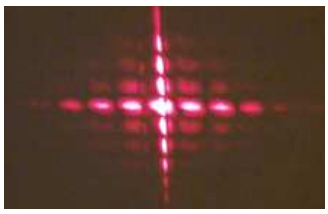

Figure 17 Diaphragm rotates 45^0

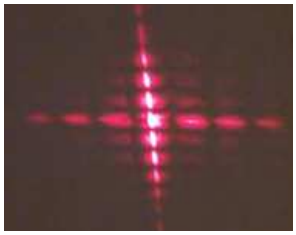

Figure 18 Diaphragm rotates 60^0

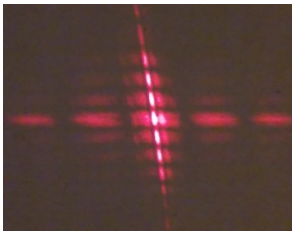

Figure 19 Diaphragm rotates 75^0

Figure 17, 18 and 19 show the interference pattern of the diaphragm rotating 45^0, 60^0 and 75^0 around Z-axis.

Observation: (1) The double slit-AB creates the expanded interference patterns; (2) the interference pattern created by double slit-CD is curved; which is the same as the phenomena shown in Section 3.

Conclusion: the interference patterns are curved and expanded simultaneously in the same experiment, attributing to the rotation of the diaphragm.

4.2. Curved, Expanded and Inclined Interference Patterns: Taking Place Simultaneously

To study the phenomena that the interference patterns are curved, expanded and inclined simultaneously in the same experiment, we use the apparatus of three double slits crossing at the same spot, one is a vertical double slit, one is horizontal, and one is tilted.

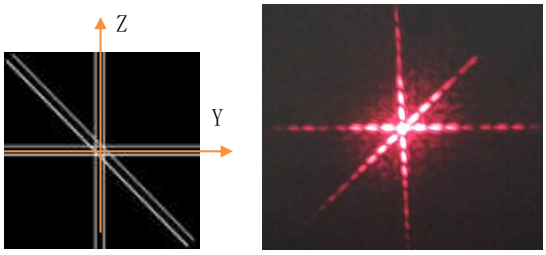

Figure 20 Diaphragm and its original interference pattern

Let us rotate the diaphragm around Z-axis counterclockwise.

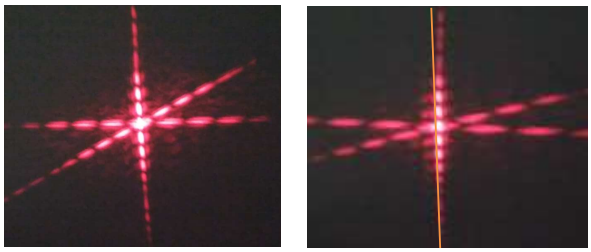

. (a) (b)

Figure 21 Diaphragm Rotate 60 degrees (a) and 75 degrees (b)

Observation: the larger the angle of the diaphragm rotates, the more inclination of the interference pattern created by the tilted double slit, the more expansion of the horizontal interferences, and the vertical interference pattern curved more. The orange-colored line in Figure 21b is to show that the patten is curved.

We show, the first time, that the interference patterns distributed along curves, inclined and expanded, attributing to the rotation of the diaphragm. The curved distribution of the fringes is different from Talbot effect and the curved Airy beam.

5. Experiments of Grating

In the grating experiments we utilized the grating of 80 slits/cm (Figure 1c).

5.1. Curved Interference Patterns

Let us rotate the grating around Y-axis (Figure 22a) clockwise, and then, counterclockwise. We observed the different curved diffraction patterns.

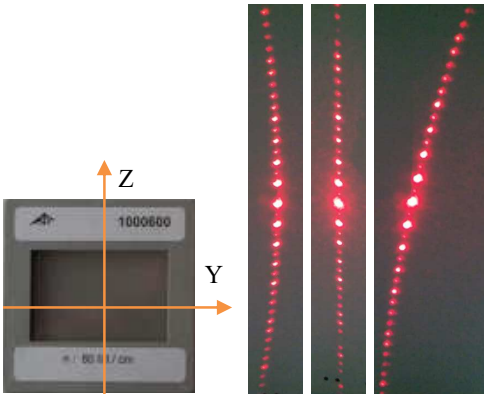

. (a) (b) (c) (d)

Figure 22 rotating grating clockwise and counterclockwise

Observation: Figure 22c shows the diffraction pattern of the diaphragm rotates 0 degree. Figure 22b shows the diffraction pattern created by the clockwise rotation of the grating. Figure 22d shows the diffraction pattern created by the counterclockwise rotation of the grating.

5.2. Expanded Interference Pattern

Figure 23a shows the diffraction pattern before the diaphragm rotating. Now rotating the grating around Z-axis 60^0 (Figure 23b).

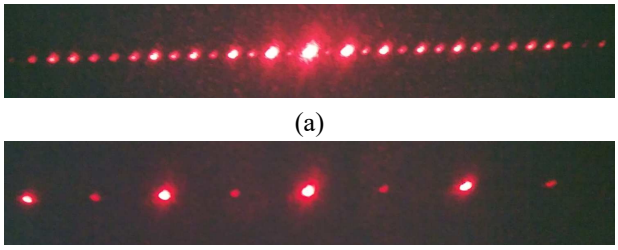

(a)

(b)

Figure 23 Expanded diffraction pattern

Observation: Figure 23b shows the expanded pattern attributing to the rotation of the grating.

5.3. Curved, Inclined and Expanded Interference Pattern

To observe the diffraction patterns that are curved, expanded and inclined simultaneously in the same experiment, we rotate the grating around A-axis that is at an angle from Y-axis (Figure 24a).

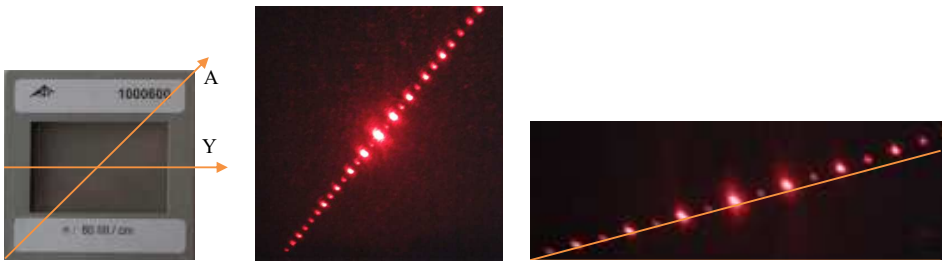

. (a) (b) (c)

Figure 24 Curved, expanded and inclined diffraction pattern

Observation: Figure 24b shows the diffraction pattern at the diaphragm's original orientation. Figure 24c shows the curved, expanded and inclined diffraction pattern due to the rotation of the grating. The tilted orange line shows that the pattern is curved. The expansion and inclination of the diffraction pattern are obvious from the comparison between Figure 24 b and 24c.

5.4. Grating Rotates Continuously: Videos

The above experiments show the patterns when the diaphragms rotate discrete angles. The videos in Appendixes show how the patterns vary continuously.

Appendix-3: Video shows that the diffraction pattern curves when the grating is rotating around Y-axis (Figure 22a). Start from the original orientation of the grating, namely, the laser beam is perpendicular to the plane of the grating. The original interference pattern is shown. Then rotating the grating around Y-axis counterclockwise. The interference pattern curves gradually and continuously. The pattern curves towards right. Then go back to the original orientation and rotate the grating again, but clockwise. The interference pattern curves again, but to opposite direction, namely, towards left.

Appendix-4: Video shows that the diffraction pattern expands when the grating is rotating around Z-axis (Figure 22a). **S**tart from the original orientation of the grating. The original interference pattern is shown. Then rotating the grating around Z-axis counterclockwise. The interference pattern expands gradually and continuously, namely the distances between fringes are gradually increased. Then go back to the original orientation and rotate the grating clockwise. The interference pattern expands again. The experiments show that the expansions of the pattern are not related with the direction of the rotation. This phenomenon is interesting and the formular is derived in next section.

Appendix-5: Video shows how the diffraction patterns curved, expanded and inclined simultaneously when the grating is rotating around A-axis (Figure 24a). Start from the original orientation of the grating. The original interference pattern is shown. Then rotating the grating around A-axis counterclockwise. The diffraction patterns vary gradually in three aspects continuously and simultaneously: First aspect, the whole pattern is inclined towards the horizontal axis. Second aspect, the distances between fringes are expanded. Third aspect, the patterns curve downwards.

Then go back to the original orientation and rotate the grating clockwise. The diffraction patterns still vary in three aspects: The whole pattern is inclined towards the horizontal axis, and the distances between fringes are expanded. Third aspect, the patterns curve, but to opposite direction, upward.

The first and second aspects have been explained mathematically in next section. However, these phenomena are interesting and challenge to interpret all consistently.

6. Description

6.1. Left-Hand Rule and Right-Hand Rule for Curved Patterns

Attribute to the rotations of the diaphragm, either clockwise or counterclockwise, the interference patterns curved. We need to determine the directions the patterns curved towards first.

6.1.1. Left-hand Rule and Right-hand Rule

The experiments above show complex interference patterns that show the curved interference patterns. To determine the direction of the interference patterns curved towards, the Left-hand Rule and Right-hand Rule were proposed [22].

Left-hand Rule: For the curved pattern created by diaphragm rotating counterclockwise.

To determine the direction of the patterns curved towards, point the left thumb to the source, the index finger is aligned with the direction of the original pattern, and the middle finger will point in the direction of the patterns curved towards, which is attribute to the counterclockwise rotation of the diaphragm (Figure 25).

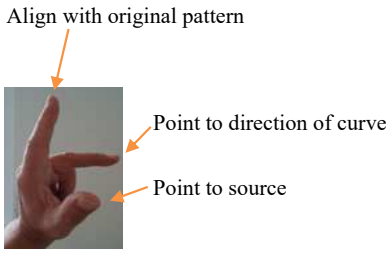

Figure 25 Left-hand Rule

Right-hand rule: For the curved pattern created by diaphragm rotating clockwise.

To determine the direction of the patterns curved towards, point the right thumb in the direction of the source, the index finger is aligned with the direction of the original pattern, and the middle finger will point in the direction of the patterns curved towards, which is attribute to the clockwise rotation of the diaphragm (Figure 26).

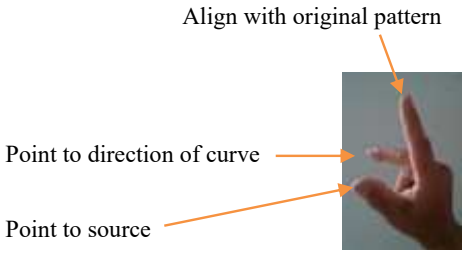

Figure 26 Right-hand Rule

6.1.2. Testing Left-hand Rule and Right-hand Rule

Next, we show that the experiments above obey Left-hand Rule and Right-hand Rule.

Figure 3: Rotating the double slit-AB clockwise with different discrete angles.

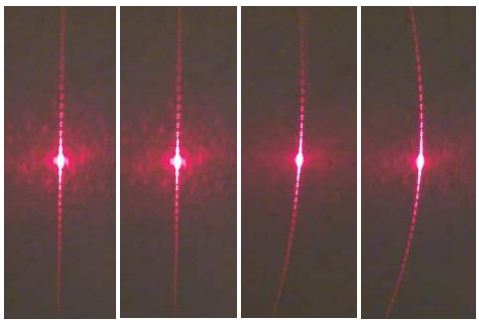

Figure 3 Curved Interference patterns

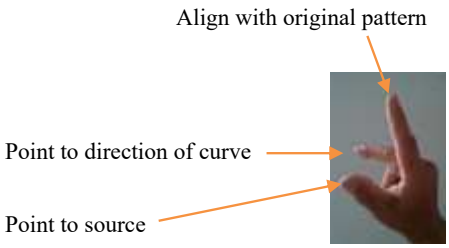

Figure 26 Right-hand rule

The lift picture of Figure 3 shows its original vertical interference pattern of the double slit experiments. For rotating clockwise, applying Right-hand rule (Figure 26). The middle finger points to the left that is the direction of the patterns curved towards.

Figure 4: rotating the double slit counterclockwise with different discrete angles.

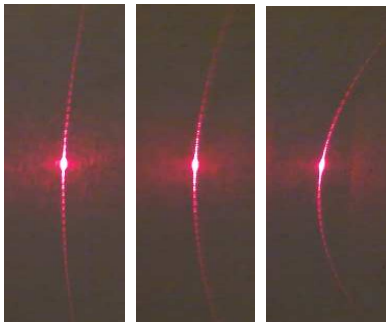

Figure 4 Curved Interference patterns

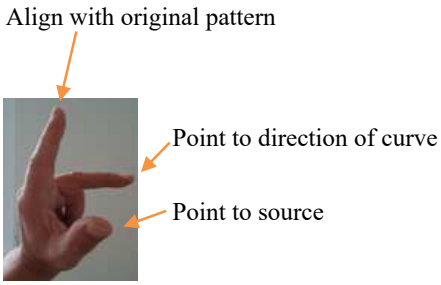

Figure 25 Left-hand rule

For rotating counterclockwise, applying Left-hand rule (Figure 25). The middle finger points to the right that is the direction of the patterns curved towards.

Figure 11: rotating the diaphragm counterclockwise.

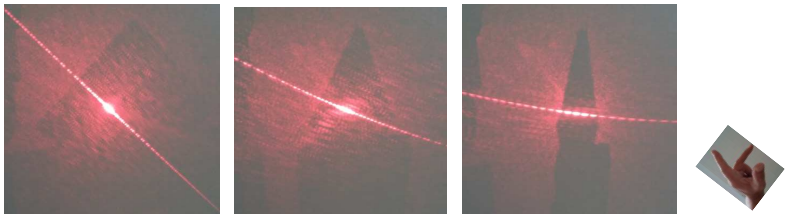

Figure 11 Rotating diaphragm counterclockwise

For rotating counterclockwise, applying Left-hand rule. The middle finger points to the up-right that is the direction of the patterns curved towards.

Figure 12: rotating the diaphragm clockwise.

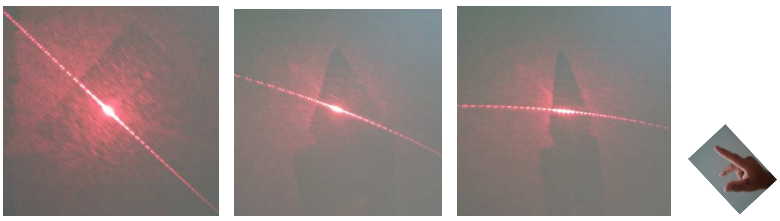

Figure 12 Rotating diaphragm clockwise

For rotating clockwise, applying Right-hand rule. The middle finger points to the down-right that is the direction of the patterns curved towards.

Figure 13: rotating the diaphragm counterclockwise.

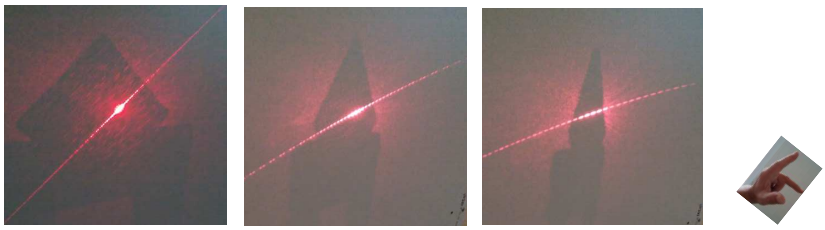

Figure 13 Rotating diaphragm counterclockwise

For rotating counterclockwise, applying Left-hand rule. The middle finger points to the down-right that is the direction of the patterns curved towards.

Figure 14: rotating the diaphragm clockwise.

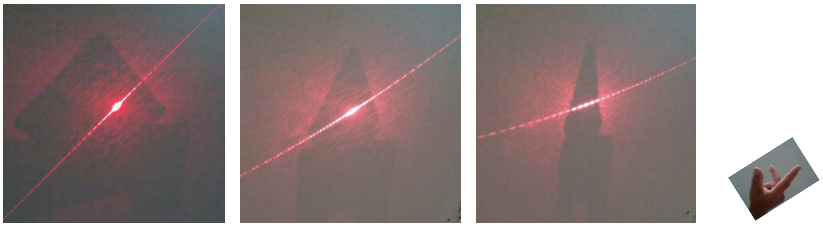

Figure 14 Rotating diaphragm clockwise

For rotating clockwise, applying Right-hand rule. The middle finger points to the up-right that is the direction of the patterns curved towards.

Figure 22: rotating the grating clockwise (Figure 22b). The direction of the curve is predicted by the Right-hand rule. To rotate the grating counterclockwise (Figure 22d), the direction of the curve is predicted by the Left-hand rule.

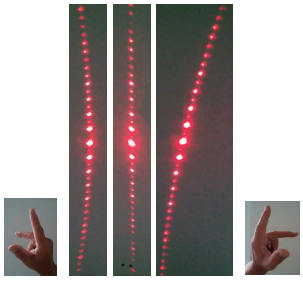

. (b) (d)

Figure 22 Curved diffraction patterns of grating

To determine the direction of the curved interference patterns, Left-hand Rule and Right-hand Rule are proposed. The experiments in this article obey the rules. However, the underlying physics of the Rules is unclear.

6.2. Formular for Expanded Patterns

6.2.1. Derivation of Formular

Let us start with Figure 2. The double-slit-AB is in the y-z plane, slit A and slit B are along the z-direction, its normal vector is along the x-axis and points to source, the coordinates of slit-A and slit-B are $y_A = d/2$ and $y_B = -d/2$, the spacing between slits A and B is "d".

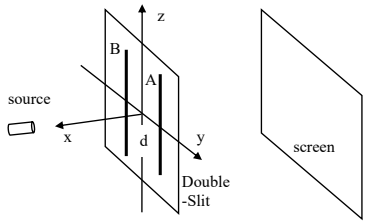

Figure 2 Setup of double slit experiment

The schematic drawing is the following.

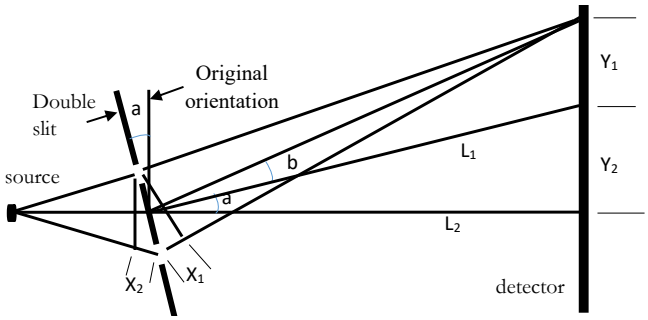

Figure 27 Schematic drawing for derivation of orientation-dependence of double slit experiments

The path difference between two waves passing through two slits respectively is $(x_1 + x_2)$. The requirement of the interference of two waves is that the path difference satisfies the following relation,

$$x_1 + x_2 = m\lambda, \quad (1)$$

where,

$$x_1 \approx dsin\angle b, \quad (2)$$

$$x_2 \approx dsin\angle a, \quad (3)$$

$$sin\angle a = \frac{y_2}{L_1} = \frac{y_2}{\sqrt{L_2^2+y_2^2}} = \frac{y_2}{L_2}\frac{1}{\sqrt{1+y_2^2/L_2^2}}, \quad (4)$$

$$sin\angle b \approx tan\angle b \approx \frac{y_1}{L_1}. \quad (5)$$

Substituting Eqs. (2), (3), (4) and (5) into Eq. (1), the equations of the orientation-dependence of the constructive/destructive interference pattern of the double slit are [14],

$$y \equiv y_1 + y_2 = \frac{m\lambda}{d}L_2\sqrt{1+(tan\angle a)^2}, \quad (6)$$

$$y = (m+\frac{1}{2})\frac{\lambda}{d}L_2\sqrt{1+(tan\angle a)^2}, \quad (7)$$

where, $(tan\angle a)^2 = \frac{y_2^2}{L_2^2}$, "y" is the position of a bright/dark fringe from the zeroth-order fringe.

6.2.2. Testing Formular

Figure 5: The diaphragm is at the original position, $\angle a = 0^0$, Eq. (6) becomes the normal formular, $y = \frac{m\lambda}{d}L$.

Figure 6: The diaphragm rotates 45^0, Eq. (6) gives $y \approx 1.4\frac{m\lambda}{d}L_2$.

Figure 7: The diaphragm rotates 60^0, Eq. (6) gives $y \approx 2\frac{m\lambda}{d}L_2$.

Figure 8: The diaphragm rotates 75^0, Eq. (6) gives $y \approx 3.86\frac{m\lambda}{d}L_2$.

Taking into account the measurement accuracy, the experiments support the formular.

Note that:

(1) the traditional formular, $y = \frac{m\lambda}{d}L$, is for a special situation that the light source is located on the normal vector of the diaphragm, but the double slit can be at any orientation on the diaphragm;

(2) the derived formular, $y = \frac{m\lambda}{d}L_2\sqrt{1 + (tan\angle a)^2}$, is for special situations that the double slit parallels to the rotation axis, but the diaphragm can be at any orientation with an angle $\angle a$;

(3) the general formular should be for the situations that the double slit can be at any orientation on the diaphragm, and the diaphragm can be at any orientation.

6.3. Formular for Inclined Interference Patterns

6.3.1. Derivation of Formula

The phenomena take place when the diaphragms rotate, we expect that the formula relates with two angles: one is the original angle of the double slit relative to the rotation axis, another is the rotation angle of the diaphragm. The mathematical formula should describe the inclination of the interference patterns of the double slit experiments. Now we study the effects for two configurations.

Configuration-1:

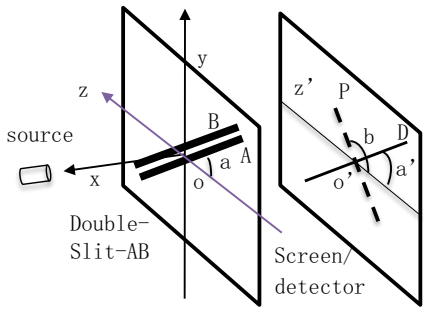

Figure 28 Schematic of Inclination of Double Slit Experiment-1

The double slit-AB is in the Y-Z plane of the diaphragm. The source is on X-axis. The angle $\angle$a is the original angle between the double alit-AB and Z-axis. Z'-axis is the projection of Z-axis on the detector. The "P" represents the interference pattern formed on the detector. The "D" represents the projection of the double slit-AB on the detector. The interference pattern "P" is perpendicular to the projection "D".

The angle ∠b is the angle between “P” and Z’-axis. The angle ∠a’ is the angle between “D” and Z’-axis. At the original orientation of the diaphragm, ∠a’ is equal to the ∠a. We have

$$\angle b = 90^0 + \angle a'$$

To describe mathematically, pick an arbitrary point “m” on the “D”, making a line mq perpendicular to Z’-axis and meets Z’-axis at the point “q”, the line o’q is the projection of the line o’m on Z’-axis. The angle $\angle mo'q$ is $\angle a'$ (Figure 29).

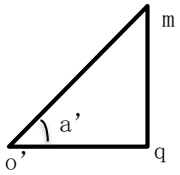

Figure 29 Schematic of projection of double slit on detector before rotating

We have,

$$\frac{mq}{o'q} = tan\angle a'$$

When the diaphragm rotates around Y-axis counterclockwise, the point “m” rotates to the point “m’ ” (Figure 30).

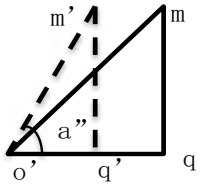

Figure 30 Schematics of projection of double slit on detector after rotating counterclockwise

The vertical length of the line mq keeps the same, i.e., $mq = m'q'$, but the line $o'q$ becomes the line $o'q'$ that is shorter then $o'q$, $o'q > o'q'$. The line $o'q$ represents the projection of the “D” on Z’-axis. The angle $\angle m'o'q'$ is the angle between the projection of the “D” and Z’-axis. The $\angle mo'q$ becomes $\angle m'o'q$, denoted as $\angle a$". We have $\angle m'o'q' > \angle mo'q$, $\angle mo'q = \angle a' = \angle a$, $\angle a" > \angle a'$, and

$$tan\angle m'o'q' = \frac{m'q'}{o'q'} = \frac{mq}{o'q'}$$

Or

$$o'q' = \frac{mq}{tan\angle m'o'q'}. \quad (8)$$

The interference pattern is perpendicular to the projection of the double slit. Now the angle between the interference pattern “P” and Z’-axis is

$$90^0 + \angle m'o'q' > 90^0 + \angle a. \quad (9)$$

The larger the diaphragm’s rotation angle, the shorter the line $o'q'$ and the larger $\angle m'o'q'$. Thus,

the interference pattern inclines to Z'-axis when the diaphragm rotates.

Next to derive the mathematical formula.

Since $mq = m'q'$, to find the $\angle m'o'q'$, we need to find $o'q'$. For this aim, let us draw the projections of the line o'm' on the X-Z-plane, denoted as the line o'q". the angle of the "D" rotated counterclockwise is $\angle q"o'q'$ or $\angle e$ (Figure 31).

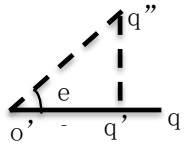

Figure 31 Schematics of projection of double slit on X-Z-plane after rotating

When the diaphragm rotates around Y-axis the angle $\angle$e, the line o'q becomes o'q", $o'q = o'q"$, and

$$cos\angle e = \frac{o'q'}{o'q"} = \frac{o'q'}{o'q}$$

$$o'q' = (o'q)cos\angle e. \tag{10}$$

Substituting Eq. (8) into Eq. (10), we obtain

$$\frac{mq}{tan\angle m'o'q'} = (o'q)cos\angle e. \tag{11}$$

Since $\frac{mq}{o'q} = tan\angle a$, substituting it into Eq. (11) we have

$$cos\angle e = \frac{tan\angle a}{tan\angle m'o'q'}.$$

Therefore

$$tan\angle m'o'q' = \frac{tan\angle a}{cos\angle e}. \tag{12}$$

The angle of the pattern relative to the Z-axis is [23]

$$90^0 + \angle m'o'q' = 90^0 + \text{act}\left[\tan\left(\frac{tan\angle a}{cos\angle e}\right)\right]. \tag{13}$$

The larger the rotation angle $\angle e$, the larger the angle $\angle m'o'q'$, namely the interference pattern inclining to Z'-axis. The angle between the "P" and Z'-axis is depending on the original angle $\angle a$ of the double slit-AB and the rotating angle $\angle e$ of the diaphragm.

For four extreme situations:

1) When $\angle e = 0^0$, i.e., the diaphragm does not rotate, $cos\angle e = 1$, act$\left[\tan\left(\frac{tan\angle a}{1}\right)\right] = \angle a$, $\angle m'o'q' = \angle a$. The interference pattern stays.
2) When $\angle e = 90^0$, i.e., the diaphragm rotating 90^0, $cos\angle e = 0$, act$\left[\tan\left(\frac{tan\angle a}{0}\right)\right] = 90^0$, $\angle m'o'q' = 90^0$. The interference pattern became parallel to Z-axis. Actually, this situation will not happen, since there will be no light passing through the double slit.
3) When $\angle a = 0^0$, i.e., the double slit is originally perpendicular to Y-axis, act$\left[\tan\left(\frac{tan0^0}{cos\angle e}\right)\right] = 0^0$, the interference pattern stays vertical.

4) When $\angle a = 90^0$, i.e., the double slit is originally in Y-direction, act $\left[\tan\left(\frac{tan90^0}{cos\angle e}\right)\right] = 90^0$, the interference pattern stays horizontal.

Next let us study the situation of rotating the diaphragm clockwise, the projection of the double slit, i.e., the line o'q" is the line o'q' as shown in Figure 32. So, we obtain the same Eq. 13.

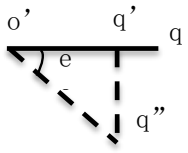

Figure 32 Schematics of the diaphragm rotating clockwise

Conclusion: The directions of the diaphragms rotate, either the clockwise or counterclockwise, have no effect on the inclination of the interference pattern.

Configuration-2: Configurataion-2 is shown in Figure 33 below:

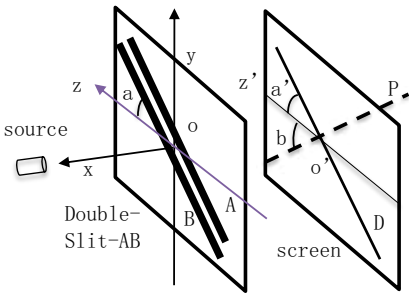

Figure 33 Schematic of Inclination of Double Slit Experiment-2

The double slit-AB is in Y-Z plane of the diaphragm. The source is on X-axis. The angle ∠a is the original angle between the double alit-AB and Z-axis. Z'-axis is the projection of Z-axis on the screen. The "P" represents the interference pattern formed on the screen. The "D" represents the projection of the double slit-AB on the screen. The "P" is perpendicular to the "D". The angle ∠b is the angle between "P" and Z'-axis. The angle ∠a' is the angle between "D" and Z'-axis. At the original orientation of the diaphragm, $\angle a'$ is equal to the ∠a. We have

$$\angle b = 90^0 - \angle a'$$

To describe mathematically, pick an arbitrary point "m" on the D, making a line mq perpendicular to Z'-axis and meets z'-axis at the point q. The line o'q is the projection of the line o'm on Z'-axis. The angle $\angle mo'q$ is $\angle a'$ (Figure 34).

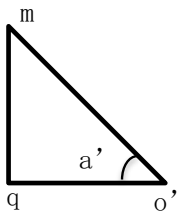

Figure 34 Schematics of projection of double slit on screen before rotating

We have,

$$\frac{mq}{o'q} = tan\angle a'$$

When the diaphragm rotates around Y-axis clockwise, the point “m” rotates to the point m’ (Figure 35).

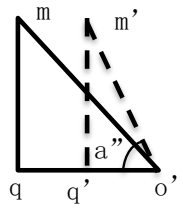

Figure 35 Schematics of projection of double slit on screen after rotating

The vertical length of the line mq keeps the same, i.e., $mq = m'q'$, but the line $o'q$ becomes $o'q'$ that is shorter then $o'q, o'q > o'q'$. The angle $\angle m'o'q'$ is the angle between the “D”, i.e., $m'o'$, and Z’-axis. The $\angle mo'q$ becomes $\angle m'o'q$, denoted as $\angle a$". We have $\angle m'o'q' > \angle mo'q$, $\angle mo'q = \angle a' = \angle a$, $\angle a" > \angle a'$ and

$$tan\angle m'o'q' = \frac{m'q'}{o'q'} = \frac{mq}{o'q'}$$

Or

$$o'q' = \frac{mq}{tan\angle m'o'q'}. \quad (14)$$

The interference pattern is perpendicular to the double slit. Now the angle between the “P” and Z’-axis is

$$90^0 - \angle m'o'q' < 90^0 - \angle a. \quad (15)$$

When the rotating angle of the diaphragm becomes larger, the $\angle m'o'q'$ becomes larger and approaches to 90^0. Therefore,

$$90^0 - \angle m'o'q' \to 0^0$$

Namely, the interference pattern inclines to the Z’-axis.

To find the mathematical description, we need to find the relation between $\angle m'o'q'$, $\angle a$ and the diaphragm’s rotation angle. Since $mq = m'q'$, to find the $\angle m'o'q'$, we need to find $o'q'$. For this aim, we draw Figure 36 that is in the X-Z plane.

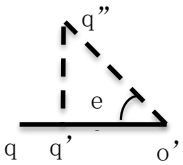

Figure 36 Schematics of projection of double slit on X-Z’-plane after rotating $\angle e$.

The $o'q''$ is the projection of the $o'm'$ on X-Z’-plane. The $o'q'$ is the projection of $o'q''$ on Z’-axis. The angle of the “D” rotated clockwise is $\angle q"o'q'$ or $\angle e$.

When the diaphragm rotates around Y-axis an angle $\angle e$ clockwise, the line $o'q$ becomes $o'q''$, i.e., $o'q = o'q$", and

$$cos\angle e = \frac{o'q'}{o'q"} = \frac{o'q'}{o'q}$$

$$o'q' = (o'q)cos\angle e. \tag{16}$$

Substituting Eq. (14) into Eq. (16), we have

$$(o'q)cos\angle e = \frac{mq}{tan\angle m'o'q'}. \tag{17}$$

Since $\frac{mq}{o'q} = tan\angle a$, Eq. (17) gives

$$cos\angle e = \frac{tan\angle a}{tan\angle m'o'q'}$$

Therefore

$$tan\angle m'o'q' = \frac{tan\angle a}{cos\angle e}. \tag{18}$$

The angle of the interference pattern relative to the Z-axis is [23],

$$90^0 - \angle m'o'q' = 90^0 - \text{act}\left[\tan\left(\frac{tan\angle a}{cos\angle e}\right)\right]. \tag{19}$$

The larger the rotation angle $\angle e$, the larger the angle $\angle m'o'q'$, namely the interference pattern inclining to Z'-axis more. The angle between the interference pattern and Z'-axis is depending on the original angle $\angle a$ of the double slit-AB and the rotating angle $\angle e$ of the diaphragm.

For four extreme situations:

1) When $\angle e = 0^0$, i.e., the diaphragm does not rotate, $cos\angle e = 1$, $\text{act}\left[\tan\left(\frac{tan\angle a}{1}\right)\right] = \angle a$, $\angle m'o'q' = \angle a$. The interference pattern is the original one.
2) When $\angle e = 90^0$, i.e., the diaphragm rotating 90^0, $cos\angle e = 0$, $\text{act}\left[\tan\left(\frac{tan\angle a}{0}\right)\right] = 90^0$, $\angle m'o'q' = 90^0$. The interference pattern became parallel to Z-axis. Actually, this situation will not happen, since there will be no light passing through the double slit.
3) When $\angle a = 0^0$, i.e., the double slit is originally perpendicular to Y-axis, $\text{act}\left[\tan\left(\frac{tan0^0}{cos\angle e}\right)\right] = 0^0$, the interference pattern stays vertical.
4) When $\angle a = 90^0$, i.e., the double slit is originally in Y-direction, $\text{act}\left[\tan\left(\frac{tan90^0}{cos\angle e}\right)\right] = 90^0$, the interference pattern stays horizontal.

Next let us rotate the diaphragm counterclockwise, the "D", i.e., o'q", is shown in Figure 37. the projection of the o'q" is the o'q' that is the same as that in Figure 36. Therefore, we will obtain the same mathematical expression, Eq. 19.

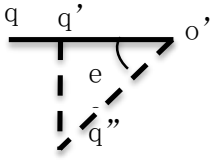

Figure 37 Schematics of the diaphragm rotating counterclockwise

Conclusion: The directions of the diaphragms rotate, either the clockwise or counterclockwise, have no effect on the inclination of the interference pattern.

Note that the formulars, Eq. 13 and Eq. 19, are for the general situation that the double slit can be at any orientation on the diaphragm, and the diaphragm can be at any orientation.

6.3.2. Testing Formular

Now test the mathematical formulars with existing experiments/observations, in which the original angle between the double slit and Y-axis is $\angle a = 45^0$. Then rotating the diaphragms 60^0 and 75^0 respectively. There are two configurations.

Configuration-1: shown by Figure 28.

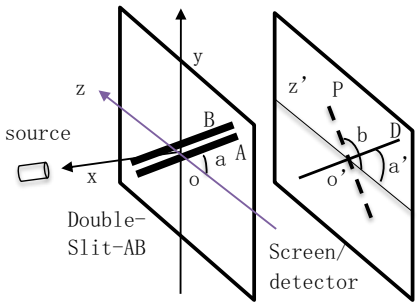

Figure 28 configuration-1

First, define how to measure the angle of the curved interference patterns: 1) drawing a line connecting the same-order fringes, for example, the green inclined lines in the following Figures. Then draw a horizontal line representing Z'-axis. The angle between those two lines is the inclination angle of the interference pattern relative to Z'-axis.

Rotating the diaphragm around Y-axis counterclockwise: (b) 60^0; (c) 75^0 (Figure 38). The angles between the interference patterns and Z-axis are shown by green lines.

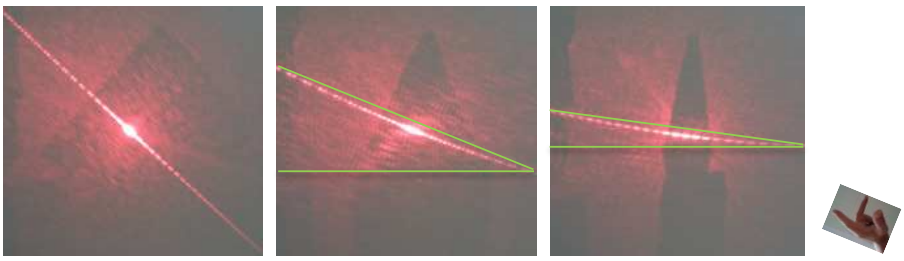

.(a) (b) (c)

Figure 38 Rotating diaphragm around Y-axis counterclockwise: (b) 60^0; (c) 75^0

Observation: the large the rotation angle of the diaphragm, the interference patterns inclined closer to the horizontal axis. The interference pattern curved upwards, which agree with Left-hand Rule.

Rotating the diaphragm around Y-axis clockwise: (b) 60^0; (c) 75^0 (Figure 39). The angles between the interference patterns and Z-axis are shown by the green lines.

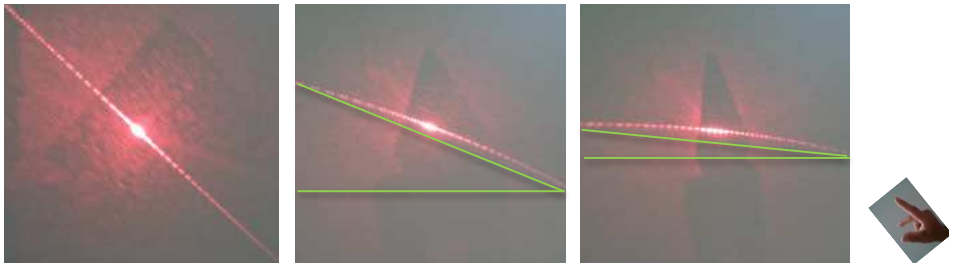

.(a) (b) (c)

Figure 39 Rotating diaphragm around Y-axis clockwise: (b) 60^0; (c) 75^0

Observation: the large the rotation angle of the diaphragm, the interference patterns inclined closer to the horizontal axis. The interference pattern curved downwards, which agree with Right-hand Rule.

Eq. (13) predicts that the inclined angles of the interference patterns, attribute to the diaphragm rotating 60^0 and 75^0, are 153^0 and 165^0, respectively, either clockwise or counterclockwise,

$$\angle b = 90^0 + \angle a' = 153^0 \text{ (For rotating } 60^0\text{)}$$

$$\angle b = 90^0 + \angle a' = 165^0 \text{ (For rotating } 75^0\text{)}$$

Configuration-2: shown by Figure 33.

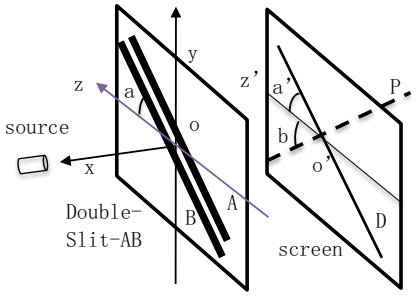

Figure 33

We have done the experiments and observed the following.

Rotating the diaphragm around Y-axis counterclockwise: (b) 60^0; (c) 75^0 (Figure 40). The angles between the interference patterns and Z-axis are shown by the green lines.

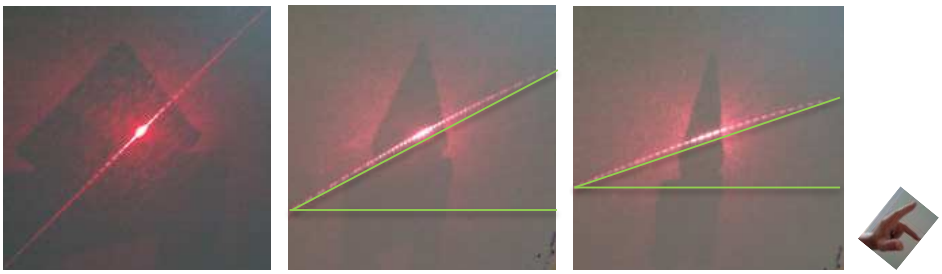

. (a) (b) (c)

Figure 40 Rotating diaphragm around Y-axis counterclockwise: (b) 60^0; (c) 75^0

Observation: the large the rotation angle of the diaphragm, the interference patterns inclined closer to the horizontal axis. The interference pattern curved downwards, which agree with Left-hand Rule.

Rotating the diaphragm around Y-axis clockwise: (b) 60^0; (c) 75^0 (Figure 41). The angles between the interference patterns and Z-axis are shown by the green lines.

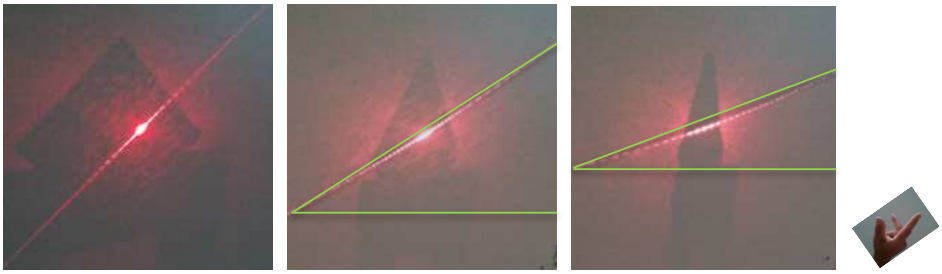

.(a) (b) (c)

Figure 41 Rotating diaphragm around Y-axis clockwise: (b) 60^0; (c) 75^0

Observation: the large the rotation angle of the diaphragm, the interference patterns inclined closer to the horizontal axis. The interference pattern curved upwards, which agree with Right-hand Rule.

Eq. (19) predicts that the inclined angles of the interference patterns, attribute to the diaphragm rotating 60^0 and 75^0 either clockwise or counterclockwise respectively, are 27^0 and 15^0 respectively,

$$\angle b = 90^0 - \angle a' = 27^0 \quad \text{(For rotating } 60^0\text{)}$$

$$\angle b = 90^0 - \angle a' = 15^0 \text{ (For rotating } 75^0\text{)}$$

Conclusion: take into account the measurement accuracy, it is reasonable to suggest that the experiments/observations support the mathematical formulas derived. More accurate experiments are needed.

By rotating the diaphragm of the double slit around one axis, we observe three phenomena simultaneously, namely, the interference patterns curved, expanded and inclined simultaneously (see attached videos, Appendix-3, -4 and -5). To determine the direction of the interference patterns curved towards, Left-hand Rule and Right-hand Rule were proposed [22]. The experiments obey the rules. However, the underlying physics of the Rules is unclear. The mathematical formulars were derived for calculating the inclination angles of the interference patterns [23], attribute to the rotations of the diaphragms. The inclination angles depend on both the original angle of the double slit relative to the rotation axis and the rotation angles of the diaphragm.

The experimental observations support the formulars.

7. Experiments: Particle or Wave

To study wave-particle duality and complementarity principle, let us define the term, “the same experiment”, as followings: when there is “only one source” emitting light/photons, regardless of the configurations of the experimental apparatus, the experiment is defined as the same experiment.

To study the double slit experiments, the “Virtual Box” model and two postulations were proposed [24] [25]. Let us divide the model into 3 zones: zone-1 (Z-1) is from the source to the diaphragm that is the left boundary of the Virtual Box; the Virtual Box is zone-2 (Z-2); and zone-3 (Z-3) is from the right boundary of the Virtual Box to the detector. The “Virtual Box” represents the diaphragms of the double slit/cross-double slit/grating and their right-side neighborhood (Figure 42).

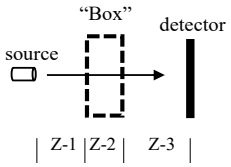

Figure 42 Double slit Apparatus with “virtual box”

Postulate-1 states that, in zone-1, photons behave as particles.

Postulate-2 states that, in zone-3, photons behave as particles. Postulate-2 predicts that in zone-3, each fringe is formed independently and can be formed partially.

Indeed, the experiments support the postulate-1 and postulate-2, but it is for the special situation that the light source is on the normal vector of the diaphragms.

Now, we study the generalized model of “Virtual Box”. In above experiments of this article, the orientations of the diaphragms vary. The generalized models are shown in Figure 43.

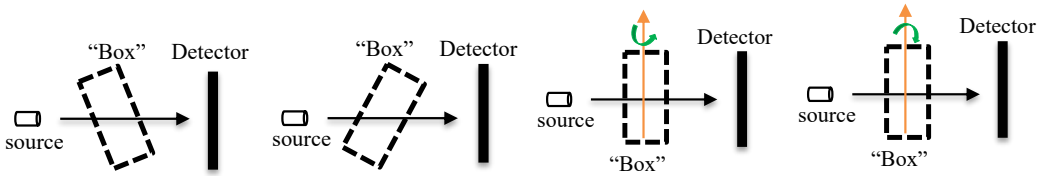

. (a) (b) (c) (d)

Figure 43 Generalized Models of Virtual Box

Figure 43a and 43b show the tilted virtual boxes, while Figure 43c and 43d show the rotating virtual boxes, where the green-colored circular arrows indicate the directions of the rotations, counterclockwise and clockwise, the orange-colored arrows indicate the rotation axis.

7.1. Blocking Curved Interference Patterns

The different orientations of the diaphragms/grating create curved, expanded and inclined interference/diffraction patterns, which corresponding to the generalized Virtual Box.

Let us block the curved patterns first. Figure 44 shows the experimental setup.

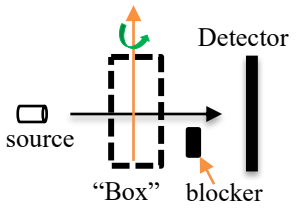

Figure 44 Experimental setup

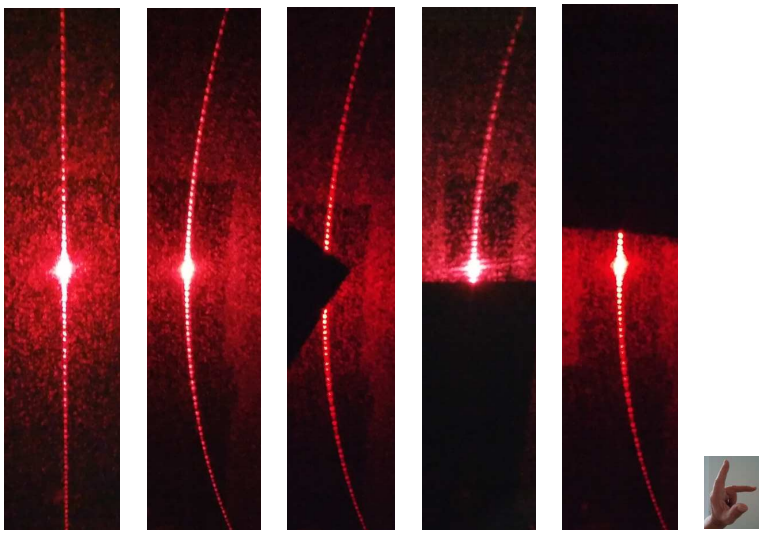

. (a) (b) (c) (d) (e)

Figure 45 Blocking Curved Patterns

Figure 45a shows the pattern created by the grating when it is at the original orientation. Figure 45b shows the pattern created by the grating when it rotates 60 degrees counterclockwise.

Next, blocking the zeroth-order fringe (Figure 45c), blocking the bottom half of the curved pattern (Figure 45d), blocking the top half of the curved pattern (Figure 45e).

Observation (Figure 45): when parts of the curved patterns are blocked, the rest parts of the patterns keep no change.

Conclusion: The fringes of the patterns are created independently and partially. Only particle can behave in such way. Postulate-2 is confirmed experimentally again: in zone-3, photons move along predetermined trajectories to form fringes and thus, behave as particles.

It is a challenge to consistently interpret the experiments.

7.2. Blocking Expanded Interference Patterns

Let us block the expanded patterns. The setup is the same as shown in Figure 44.

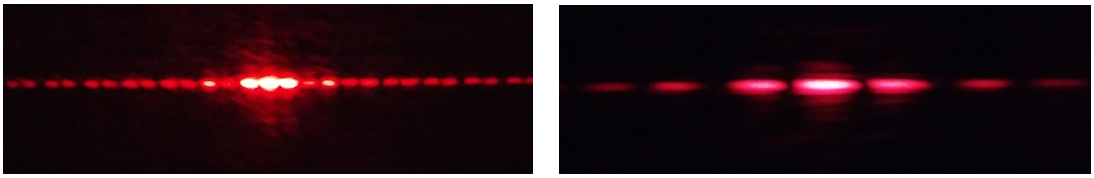

. (a) pattern of original orientation (b) pattern when grating rotates 60^0

Figure 46 Original pattern and pattern of rotating 60^0

Figure 46 shows the original pattern of the grating and expanded pattern of grating after rotating 60^0.

Let us block the pattern at different parts.

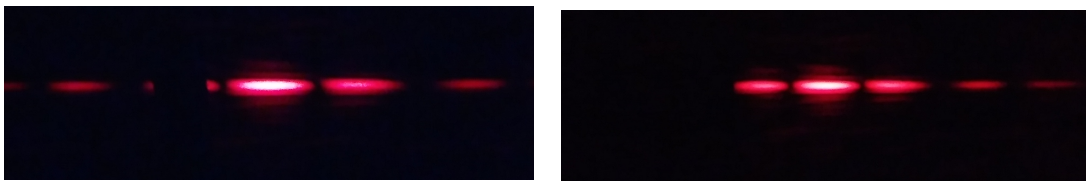

(a) Blocking first-order fringe of expanded pattern (b) blocking the left-half fringes of pattern

Figure 47 Blocking Expanded Patterns

Observation (Figure 47): when parts of the expanded patterns are blocked, the rest parts of the patterns keep no change.

We have the consistent conclusion.

Conclusion: The fringes of the patterns are created independently and partially. Only particle can behave in such way. Postulate-2 is confirmed experimentally: in zone-3, photons move along predetermined trajectories to form fringes and thus, behave as particles.

7.3. Blocking Inclined Interference Patterns

Let us block the inclined patterns. The experimental setup is the same as Figure 44. To show the inclined pattern, we have to use the tile double slit. However, the tilt double slit must create the inclined, curved and expanded pattern simultaneously (see Appendix-5). Since Figure 48 and 49 only show small portions of the pattern, the curve-feature is not shown clearly.

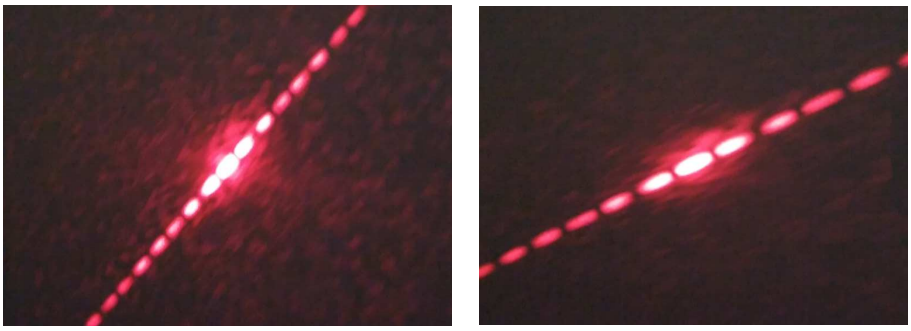

. (a) pattern of original orientation (b) pattern when grating rotates 60^0

Figure 48 Original pattern and pattern of rotating 60^0

Figure 48a and 48b show the original pattern of the grating and the inclined/expanded pattern of the grating after rotating 60^0 respectively.

Let us block the pattern at different parts.

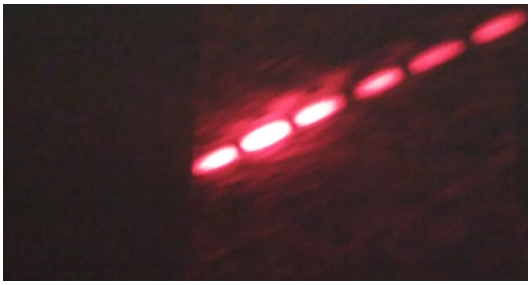

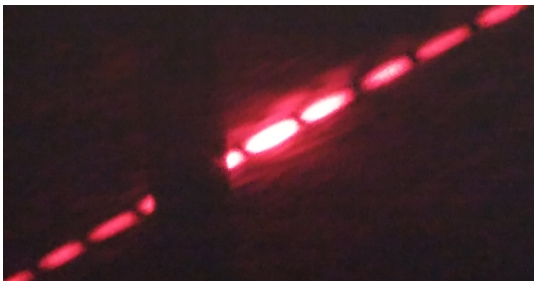

. (a) Block left-half of inclined pattern (b) Block 1st- /2nd-order fringes of inclined pattern

Figure 49 Blocking different parts of inclined/expanded patterns

Observation (Figure 49): when different parts of the inclined/expanded patterns are blocked, the rest parts of the patterns keep no change.

We have the consistent conclusion.

Conclusion: The fringes of the patterns are created independently and partially, which would be expected only if photons behave as particles in Z-3. Postulate-2 is confirmed for the grating experimentally: in zone-3, photons move along predetermined trajectories to form fringes and thus, behave as particles. Some of photons form fringes on blockers, while some of photons are distributed like partial of a wave diffraction pattern on the detector.

8. Discussion

8.1. Static Double Slit Experiments vs Dynamic Double Slit Experiments

To distinguish the regular double slit experiments and the novel double slit experiments and to understand the experiments, the regular double slit experiments are referred as the "static double slit experiments", while the novel double slit experiments are referred as "dynamic double slit experiments". The reasons are the following.

The regular double slit experiments are described by the formular,

$$y = \frac{m\lambda}{d} L.$$

Where "d" is the spacing between two slits, and is the only parameter related with the diaphragm. For a given diaphragm, i.e., the "d" is fixed, the experimental result is stationary.

On the contrary, the novel double slit/cross-double slit experiments contain three novel phenomena, curved, expanded and inclined interference patterns.

The expansion of the patterns of the novel double slit/cross-double slit experiments are described by the formular,

$$y = \frac{m\lambda}{d} L_2 \sqrt{1 + (tan\angle a)^2}. \quad (6)$$

For a given diaphragm, beside the "d", the distances between fringes are also depended on both the orientation ($\angle a$) of the diaphragm and the orientation of the double slit on the diaphragm.

The inclinations of the patterns are described by the formular,

$$90^0 + \angle m'o'q' = 90^0 + \text{act}\left[\tan\left(\frac{tan\angle a}{cos\angle e}\right)\right]. \qquad (13)$$

Eq. 13 describes that the inclinations of the patterns depend on both angles: the orientation ($\angle a$) of the double slit/cross-double slit and the angle ($\angle e$) of the diaphragm rotates.

The formular to describe the curved pattern has not been derived yet.

Namely, even with the same diaphragm, we will have the continuously changed phenomena when we simply rotate the diaphragm, i.e., the phenomena are dynamically changed. Therefore, we referred those as "dynamic double slit/cross-double slit experiments".

8.2. On Light Bending

Postulate-2 has been confirmed for the regular/static double slit experiment. In Section 7, it is shown that postulate-2 holds for novel/dynamic double slit/grating experiments, namely light beam behaves as particles before arriving at the detector and forming the curved pattern.

Based on the confirmed postulate-2, we re-study the interference/diffraction patterns of the double slit/cross-double slit/grating experiments (Figure 50).

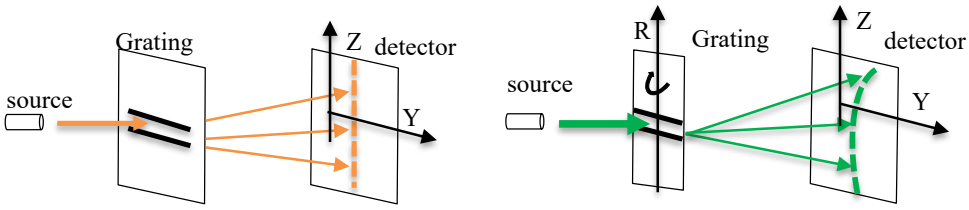

. (a) (b)

Figure 50 Normal/static vs novel/dynamic grating experiments

Photons behave as particle before land on the detector at the position of each fringe (Figure 50a). Indeed, after passing the diaphragm/grating, photons propagate as particles and land on the position of each fringe respectively, namely, photons bend along Z-direction to land on a straight line to form different fringes (orange-colored light rays and fringes) (Figure 50a).

This phenomenon is the "light bending", referred it as "straight-line light bending". Namely the "interference pattern" is the "straight-line light bending".

After passing the rotated diaphragm/grating, photons behaving as particles land on the detector along the curved line (green-colored) to form fringes (Figure 50b).

This phenomenon is the "light bending" as well, referred it as "curved-line light bending", or "curved interference pattern"

In the "curved-line light bending", the photons bend not only in the Z direction, but also in Y-direction. The net bending is the combination of both bending.

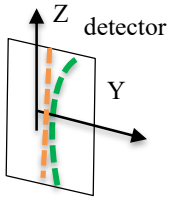

Figure 51 “Straight-line light bending” vs “Curved-line light bending”

We suggest an interpretation to explain the phenomenon of the curved pattern. A laser source emits photons as a beam of particles (as proved experimentally when testing postulate-1). Those photons travel into the virtual box.

In the language of “wave theory”, the function of the “virtual box” is a process of “forming” the distribution of photons as waves.

In the language of “particle theory”, the function of the “Virtual box” is a process of “grouping” photons into different groups/streams (denoted the process as “grouping”), which correspond to different fringes respectively. Photons landing on the same fringe are defined as “in the same group”. In practice, a “group” of photons propagates as a stream of particles and arrives at the same fringe continuously. Therefore, different groups/streams corresponding to different fringes are formed inside the virtual box. Where the process completed, either in “wave language” or in “particle language”, is defined as the right-side boundary of the virtual box.

When coming out of the “virtual box”, photons behave as groups/streams of particles (as proved experimentally when testing postulate-2), and follow the trajectories that lead to the different fringes. Although the trajectory of each photon cannot be determined, the trajectory of each group/stream of photons is determined while they are inside the “virtual box”. The trajectories of each group/stream of photons are shown by the evolution of each fringe after photons coming out the “virtual box”. However, the trajectories cannot be directly observed at the right-side boundary of the “Virtual box”, because existing observation equipment can only register photons, but cannot detect the directions of each group/stream of photons simultaneously. The right-side boundary is a point at which, different groups/streams of photons separate. One can observe the patterns only when different groups/streams of photons separate.

The mechanism of “forming” or “grouping” is mystery.

In the static double slit/cross-double slit experiments, photons are “forming” or “grouping” to propagate to the straight-line positions of the fringes, i.e., photons bended along a straight line.

In the dynamic double slit/cross-double slit experiments, photons are “forming” or “grouping” to propagate to the curved-line positions of the fringes, or to the expanded positions of the fringes, or to the inclined positions of the fringes.

The Feynman's mystery of the double slit experiments becomes more mysterious.

9. Summery

We show the new phenomena that the interference patterns of the double slit and cross-double slit experiments depend on the orientation of the diaphragms. When the diaphragms rotate: (1) around different axis; (2) clockwise or counterclockwise; (3) different angles, the photons' behaviors are significantly different: curved, expanded and inclined, or two of three phenomena, or all three phenomena, taking place simultaneously in the same experiment.

We derived the formulars to describe the expansion and inclination, and proposed Right-hand rule and Left-hand rule to determine the direction of the interference patterns curved towards.

The significances of the novel double slit and cross-double slit experiments of this article are: (1) discovered, the first time, three novel phenomena, i.e., the patterns curved, expanded and inclined; and (2) provide comprehensive phenomena/information for developing theoretical model to explore the mystery of the double slit experiments.

Let us compare the phenomena of the curved light.

	Refraction of light	Gravity bends light	Talbot effect	Curved Airy beam	Novel phenomena of this article
cause	Refractive index	gravity	Diffraction	Interfered waves	Interference
apparatus	Two mediums	Massive object	Grating	Methods/device: control waves	Double slit, cross-double slit
phenomena	Light bended	Light bended	Self-imaging, patterns distribute along tilt lines	Beams move along curved trajectory	Patterns: Curved, expanded, inclined
theory	optics	General relativity	optics	Quantum theory, Maxwell theory	
applications		Gravity lenses	acoustics, x ray, plasmonic [5]	biomedical imaging, filamentation [12]	

Three novel phenomena may be described by Maxwell's equations [26] or quantum theory. It is challenge to interpretate the experiments of the double slit/cross-double slit when the diaphragm rotating, respectively, around X-axis, Y-axis and Z-axis clockwise and counterclockwise consistently.

Appendixes:

(A1) Expanded Pattern of Disc-ring Apparatus

The disc-ring apparatus consists of the disc-3 and the ring-2. Both disc-3 and ring-2 are formed on the opaque diaphragm, denoted as the disc-ring apparatus. The diaphragm is denoted as "1" in Figure A1a. Figure A1b shows the enlarged real disc-ring apparatus.

(A1-1): Apparatus

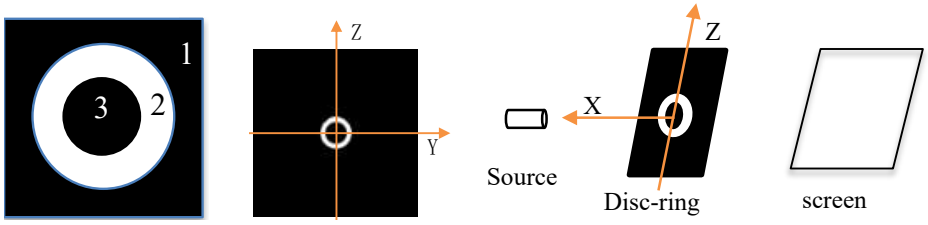

. (a) (b) (c)

Figure A1 Disc-Ring apparatus

Figure A1c shows the experimental setup: the diaphragm of the disc-ring is at its original orientation, i.e., the normal vector of the diaphragm is along X-axis, and its pattern (Figure A2).

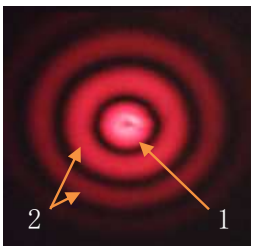

Figure A2 Disc-ring and disc-pattern: rotating 0 degree

Observation: there is the disc-shape interference pattern at the center, denoted by number "1" in Figure A2, referred to it as the disc-pattern. A brighter spot is at the center of the disc-pattern. Refer the ring-shape interference patterns as the ring-patterns, denoted by "2" in Figure A2.

The original orientation is that the light beam is perpendicular to the plane of the diaphragm.

We suggest that the formular to describe the interference patterns of the disc-ring experiments is the same as that of the regular double slit. Namely, at the original orientation, the positions of the ring-patterns are

$$y = m\frac{\lambda L}{d}. \qquad \text{(A1)}$$

Where "d" is the diameter of disc-3, "L" is the distance between the diaphragm and the screen, "y" is the position of bright ring-patterns, "m" is integers.

(A1-2): Rotating Diaphragm

Then rotate the diaphragm around Z-axis.

Figure A3 shows the patterns of the disc-ring rotating 30^0.

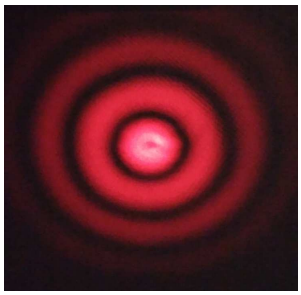

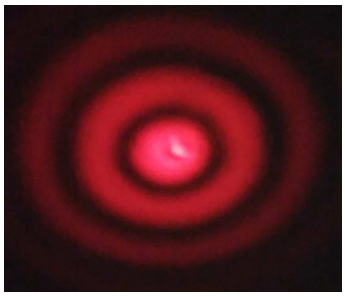

Figure A2 Diaphragm rotating 0^0 Figure A3 Diaphragm rotating 30^0

Figure A4 and Figure A5 show the patterns of the disc-ring rotating 45^0 and 60^0 respectively.

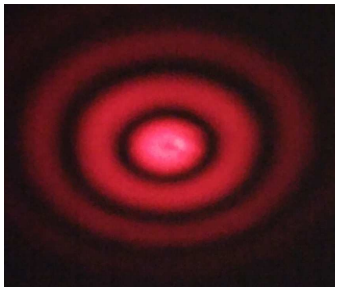

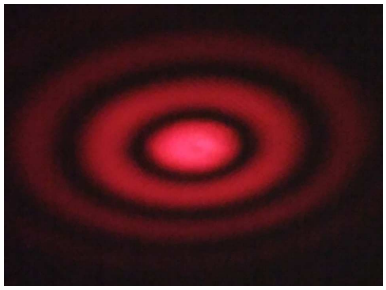

Figure A4 Rotating 45^0 Figure A5 Rotating 60^0

Figure A6 shows the patterns of the disc-ring rotating 75^0.

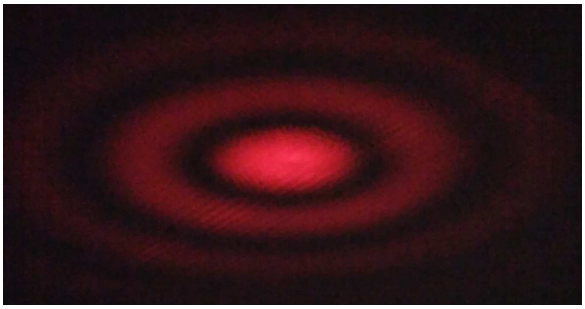

Figure A6 Diaphragm Rotating 75^0

Observation: the expansion along Y-axis is larger than that along Z-axis. There is a bright spot at the center of the disc-pattern in Figures A2, A3 and A4.

Conclusion: The larger the rotation angle of the diaphragm, the larger the expansion of the patterns.

(A1-3): Disc-Ring vs Avago Disc vs Circular Aperture

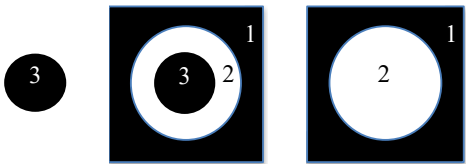

. (a) (b) (c)

Figure A7 Avago disc vs Disc-ring vs Circular aperture

Figure A7a shows Avago disc that is the circular opaque disc; Figure A7b is the disc-ring apparatus proposed in this article; Figure A7c shows the circular aperture.

The disc-ring can be considered as the combination of Avago disc and the circular aperture.

(A1-4): Disc-Pattern/Ring-Patterns vs Avago Spot vs Airy Disc/Airy Patterns

When light shines on Avago disc perpendicularly, the light passing the edge of the disc arrives at the shadow on the screen. The interference of the light creates a bright spot at the shadow's center, referred as Avago spot or Poisson spot [27] (Figure A8a).

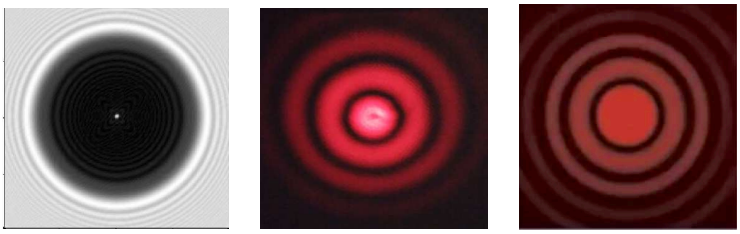

. (a) (b) (c)

Figure A8 Disc-pattern vs Avago spot vs Airy disc

Figure A8b is the disc-pattern and ring-patterns of the disc-ring apparatus at the original orientation. There is a bright spot at the center of the disc-pattern of the disc-ring.

Figure A8c shows Airy disc and Airy patterns [28].

The disc-pattern and the ring-patterns have the similar shape as that of Airy-disc and Airy-patterns.

Note that, for the disc-ring apparatus, the distances between two adjacent ring-patterns are the same. For circular aperture, however, the distances between two adjacent Airy patterns are different.

(A2) Expanded, Inclined and Curved Interference Patterns of

More Cross-Double Slit Experiments

Here we present more experiments of expanded, inclined and curved interference patterns of cross-double slit. There are same phenomena in the single slit experiments [29].

(A2-1) Two Double Slit Crossing

Figure A9 shows the setup and pattern. Figure A10 shows the expanded and inclined pattern when the diaphragm rotates around Z-axis counterclockwise.

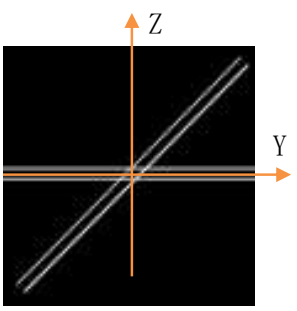

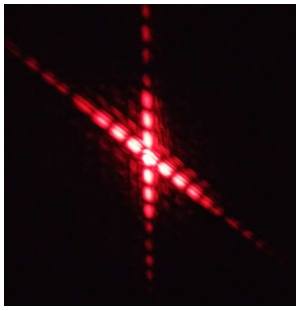

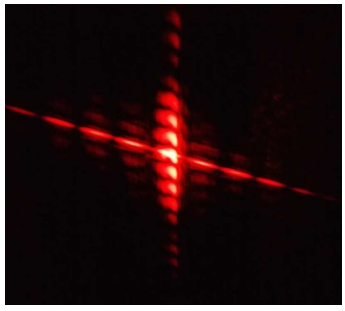

Figure A9 Cross-double slit and original pattern

Figure A10 Expanded/inclined pattern

When the diaphragm rotates around Y axis, the pattern expanded and inclined (Figure A11, A12).

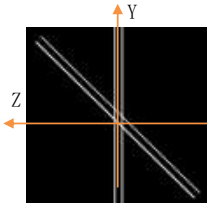

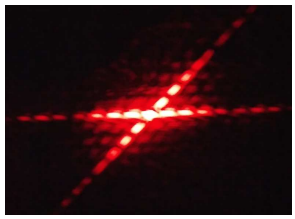

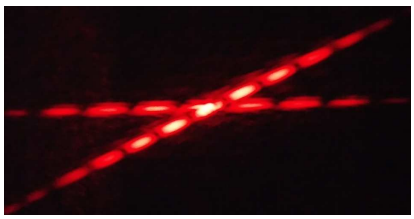

Figure A11 Original pattern

Figure A12 expanded and inclined pattern

(A2-2) Three Double Slit Crossing

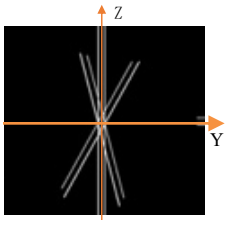

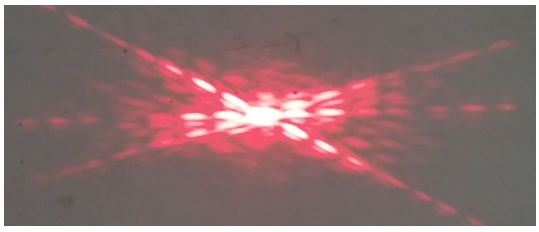

Figure A13 Original orientation: Rotating 0^0

When the diaphragm rotates, the laser source stay.

Rotating around Z-axis: Figure A14 shows the interference pattern of cross-double slit rotating 60^0.

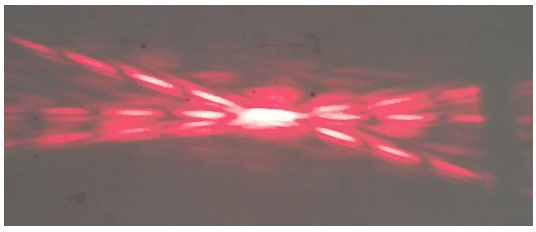

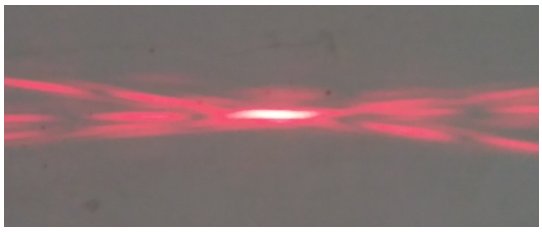

Figure A14 Rotating 60^0

Figure A15 Rotating 75^0

Figure A15 shows the interference pattern of cross-double slit rotating 75^0 around Z-axis.

Observation: (1) the larger the rotation angle, the larger the distance between fringes; (2) the interference patterns created by two tilt double slits inclined to Y-axis.

Rotating Around Y-axis:

Now we use the same diaphragm of Figure A13 but rotating around Y-axis. The vertical double slit creates the horizontal interference pattern, while two tilt double slits create two tilt interference patterns (Figure A16).

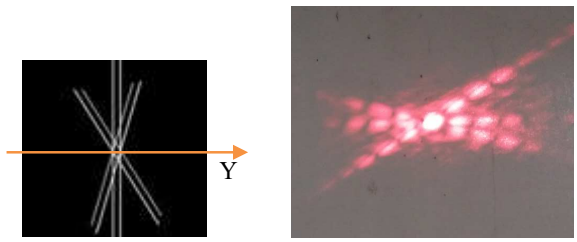

Figure A16 Rotating 0^0

Figure A17 shows the interference patterns created by the diaphragm rotating respectively 45^0 (Figure A17a), 60^0 (Figure A17b) and 75^0 (Figure A17c) around Y-axis.

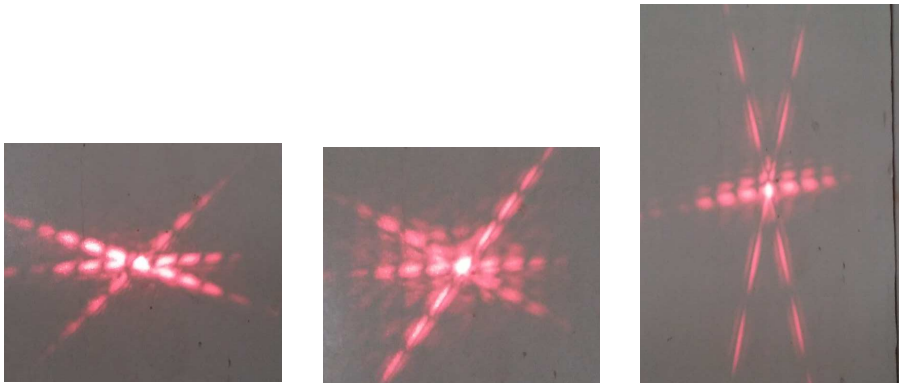

.(a) rotating 45^0 (b) rotating 60^0 (c) rotating 75^0

Figure A17 Diaphragm rotating 45^0 (a), 60^0 (b) and 75^0 (c)

Observation: (1) the interference patterns created by two tilt double slits incline to Z-axis. (2) the larger the rotation angle, the larger the distance between fringes created by the tilt-double slits.

(A2-3) Six Double Slit Crossing

Now consider a cross-double slit that consists of six double slits crossing to each other (Figure A18). The Z-axis is between two vertical slits and parallel to them. The laser source is on the normal vector of the cross-double slit at the original orientation.

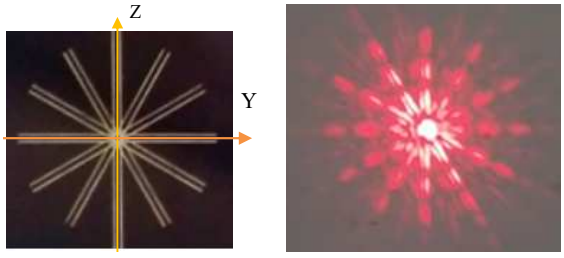

Figure A18 Cross-double slit and its pattern: Rotating 0^0

Figure A19 shows the interference pattern of the cross-double slit rotating 60^0 around Z-axis.

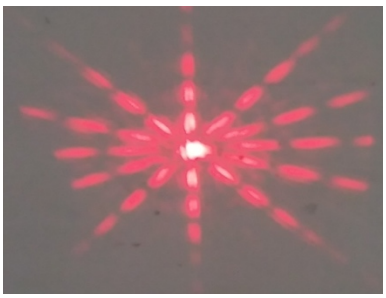

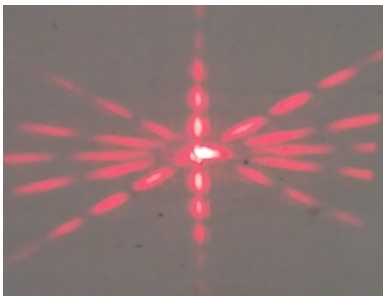

Figure A19 Rotating 60^0 Figure A20 Rotating 75^0

Figure A20 shows the interference pattern of the cross-double slit rotating 75^0 around Z-axis.

Observation: (1) the larger the rotating angle of the diaphragm, the larger the distances between two fringes created by non-horizontal double slits; (2) the distance between fringes created by the vertical double slit is largest; (3) the interference patterns created by the tilt double slits inclined to Y-axis.

We show that the interference patterns have inclined attributing to the rotation of the diaphragm. Interference patterns have expanded and inclined simultaneously in the same experiment.

(A3) Link of Video-1: Evolution of curved interference patterns.

(A4) Link of Video-2: Evolution of expanded interference patterns

(A5) Link of Video-3: Evolution of curved, expanded and inclined interference patterns

References

[1] A. I. Sabra, *Theories of Light from Descartes to Newton*, Cambridge University Press, 1981.

[2] S. Weinberg, *Gravitation and cosmology: principles and applications of the general theory of Relativity*, New York: Wiley, 1972.

[3] H. F. Talbot, "Facts relating to optical science," Philos. Mag. 9, 401–407 (1836).

[4] Lord Rayleigh, "On copying diffraction gratings and on some phenomenon connected therewith," Philos. Mag. 11, 196–205 (1881).

[5] J. Wen, Y. Zhang, and M. Xiao, "The Talbot effect: recent advances in classical optics, nonlinear optics, and quantum optics", Advances in Optics and Photonics, DOI: 10.1364/AOP.5.000083, 2013.

[6] M. V. Berry and N. L. Balazs, "Non-Spreading Wave Packets", American Journal of Physics 47(3): 264-267, DOI: 10.1119/1.11855, 1979.

[7] G. A. Siviloglou and D. N. Christodoulides, "Accelerating finite energy Airy beams," Opt. Lett. 32, 979–981 (2007).

[8] G. A. Siviloglou, J. Broky, A. Dogariu, and D. N. Christodoulides, "Observation of accelerating

Airy beams," Phys. Rev. Lett. 99, 213901 (2007).

[9] Ido Kaminer, Rivka Bekenstein, Jonathan Nemirovsky, and Mordechai Segev, "Nondiffracting Accelerating Wave Packets of Maxwell's Equations", Phys. Rev. Lett, **108**,163901, 2012

[10] F. Courvoisier, et.al., **"**Sending femtosecond pulses in circles: highly nonparaxial accelerating beams"**,** *Opt. Lett.*, **37**, Issue (10), 1736 – 1738, 2012.

[11] Jon Cartwright, "Light Bends by Itself", Science, 2012.

[12] N. K. Efremidis, et.al., "Airy beams and accelerating waves: an overview of recent advances", Optica, https://doi.org/10.1364/OPTICA.6.000686, 2019.

[13] Hui Peng, "Curved Interference Pattern", Research Square, preprint, DOI: 10.21203/rs.3.rs-677223/v1, 2021.

[14] Hui Peng, "Novel Double Slit and Cross-Double Slit Experiments--- Interference Patterns Depending on Orientation of Diaphragm", Research Square, preprint, DOI: https://doi.org/10.21203/rs.3.rs-653201/v1, 2021.

[15] A. Ananthaswamy, "Through Two Doors at Once", Dutton, New York, NY, (2018).

[16] A. Robinson, "The Last Man Who Knew Everything". New York, NY: Pi Press., (2006).

[17] R. Feynman, R. Leighton, and M. Sands, "The Feynman Lectures on Physics" (Addison-Wesley, Reading, 1966), Vol. 3.

[18] S. Rashkovskiy, "Is a rational explanation of wave-particle duality possible?" arXiv 1302.6159 [quant-ph] 2013.

[19] Hui Peng, "Observation of Cross-double slit Experiments". I*nternational J. of Physics*., 8(2), 39-41. DOI: 10.12691/ijp-8-2-1, 2020.

[20] Hui Peng, "Double Slit to Cross-Double Slit to Comprehensive Double Slit Experiments", Research Square, preprint, DOI: 10.21203/rs.3.rs-555223/v1, 2021.

[21] Personal communication with Dr. Ian Miller.

[22] Hui Peng, "Novel Double Slit Experiments: Right-hand Rule and Left-hand Rule ---Interference Patterns Curved, Expanded and Inclined Simultaneously", Research Square, preprint, DOI: https://doi.org/10.21203/rs.3.rs-737506/v1, 2021.

[23] Hui Peng, "Inclined, Expanded and Curved Interference Pattern of Double Slit Experiment ---Mathematical Description (1)", Research Square, preprint, DOI: https://doi.org/10.21203/rs.3.rs-755594/v1, 2021.

[24] Hui Peng, "Comprehensive Double Slit Experiments---Exploring Experimentally Mystery of Double Slit", Researchsquare, preprint, DOI: 10.21203/rs.3.rs-237907/v1, 2021.

[25] Hui Peng, "Experimental Study of Mystery of Double Slit---Comprehensive Double Slit

Experiments", *International Journal of Physics*", 9(2), 114-127. DOI: 10.12691/ijp-9-2-6, 2021.

[26] Personal communication with Dr. Greg Poole.

[27] Michel Gondran, Alexandre Gondran. Energy flow lines and the spot of Poisson-Arago. hal- 00416055v1, 2009.

[28] ASCPhysicsAndAstronomy

[29] Hui Peng, "Novel Universal Phenomena of Single Slit, Double Slit, Cross-double Slit and Triple Slit Experiments --- Curved Patterns and Orientation-Dependence of Patterns", Research Square, Preprint, DOI: https://doi.org/10.21203/rs.3.rs-722731/v1, 2021.

Supplementary Files

This is a list of supplementary files associated with this preprint. Click to download.

- 020210822curved.mp4
- 020210822inclinedcurvedexpand.mp4
- 020210822expand.mp4